Alexandria Engineering Journal (2023) 68, 587–609

HOSTED BY

Alexandria University

Alexandria Engineering Journal

www.elsevier.com/locate/aej
www.sciencedirect.com

REVIEW

Natural and synthetic superhydrophobic surfaces: A review of the fundamentals, structures, and applications

Freshteh Sotoudeh [a], S Mahmood Mousavi [a], Nader Karimi [b,c], Bok Jik Lee [a,*], Javad Abolfazli-Esfahani [d], Mohammad K.D. Manshadi [e]

[a] *Institute of Advanced Aerospace Technology, Seoul National University, Seoul 08826, Republic of Korea*
[b] *School of Engineering and Materials Science, Queen Mary University of London, London E1 4NS, UK*
[c] *James Watt School of Engineering, University of Glasgow, Glasgow G128QQ, UK*
[d] *Mechanical Engineering Department, Center of Excellence on Modelling and Control Systems, (CEMCS), Ferdowsi University of Mashhad, Mashhad, Iran*
[e] *Mechanical Engineering Department, Southern Methodist University, Dallas, TX 75275, USA*

Received 24 June 2022; revised 26 December 2022; accepted 26 January 2023
Available online 2 February 2023

KEYWORDS

Superhydrophobic surface;
Self-cleaning;
Water-repellent;
Contact angle

Abstract Self-cleaning surfaces are nature-inspired and based on the surface processes occurring on butterfly wings and lotus leaves. Owing to their unique characteristics, they are usable in a number of industrial applications, including the manufacture of solar panels and glass. In particular, they can be used for the separation of oil and water, which is highly relevant to petroleum technologies. Self-cleaning surfaces help to reduce the time and cost of keeping equipment clean while enhancing its durability, and they can be broadly categorized into hydrophilic and hydrophobic surfaces. On hydrophilic surfaces, water spreads considerably (sheeting of water), and therefore, it can transport contaminants and leave a clean surface. However, a hydrophobic surface is cleaned by the slipping of water droplets on it. Currently, water-repellent surfaces are used more widely in self-cleaning technologies. The selection and design of such surfaces require a thorough understanding of the underlying physical chemistry of the relevant process. This paper presents an in-depth discussion of self-cleaning surfaces, with an emphasis on their applications in the petroleum industry.

* Corresponding author.
E-mail address: b.lee@snu.ac.kr (B.J. Lee).

Peer review under responsibility of Faculty of Engineering, Alexandria University.

https://doi.org/10.1016/j.aej.2023.01.058
1110-0168

Contents

1. Introduction

Hydrophobicity and hydrophilicity are amongst the key properties of many surfaces. One of the main features of these surfaces is their self-cleaning behavior. Numerous studies have investigated the potential applications of such surfaces and their fabrication methods. This review summarizes those investigations and highlights recent advancements in the use of self-cleaning surfaces and their manufacturing processes. It indicates directions for future research and points out some potential uses of self-cleaning surfaces. Furthermore, it discusses the fundamental physics of such surfaces.

On a hydrophilic surface, water tends to spread, resulting in the formation of a thin layer of water. This phenomenon depends on the contact angle (CA) on the surface, formed at the interface of solid, liquid, and gas phases at the point where the liquid drop is in contact with the solid surface [1,2]. A hydrophilic surface has a CA lower than 90°, and surfaces with a CA close to 0° are ultra-hydrophilic. When the surface CA exceeds 90°, the surface is termed hydrophobic. Further, surfaces with a CA greater than 150° are called superhydrophobic (SH) surfaces [3].

A liquid's capability to maintain contact with the surface of a solid is referred to as wettability, and it is the net outcome of interactions among intermolecular forces [4,5]. Wettability (wetting degree) is specified on the basis of the balance between adhesive and cohesive forces. The spreading of a drop of liquid on a surface is because of adhesive forces between the liquid and solid. On the other hand, cohesive forces between water molecules tend to minimize the contact of water droplets with a surface. Regardless of wettability, the shape of a droplet on a solid surface is spherical. As mentioned, the wettability is determined by the surface CA. As shown in Fig. 1, a smaller CA leads to a higher wettability, and vice versa [6,7]. There are various kinds of solid surface wettability, such as the famous Young's model (Fig. 2a), Wenzel model (Fig. 2b), Cassie–Baxter model (Fig. 2c), and Bico and Quéré theory. The Young–Dupré equation is used to determine the structure of a liquid–vapor interface, wherein the CA has a boundary condition role through the Young equation [8]. A contact can be theoretically described by considering the thermodynamic balance among the three phases, namely liquid, solid, and gas or vapor phases (hereafter represented by the letters L, S, and G, respectively). The gas or vapor phase can be a mix of ambient atmosphere and a balanced liquid–vapor concentration. Furthermore, an immiscible liquid phase can replace the "gaseous" phase. In Fig. 2a, if γ_{SG}, γ_{SL}, and γ_{LG} denote the solid–vapor, solid–liquid, and liquid–gas surface tensions, respectively, then the Young equation can be used to calculate the equilibrium CA (θ_C) as follows [9]:

$$\gamma_{SG} - \gamma_{SL} - \gamma_{LG}\cos\theta_C = 0 \quad (1)$$

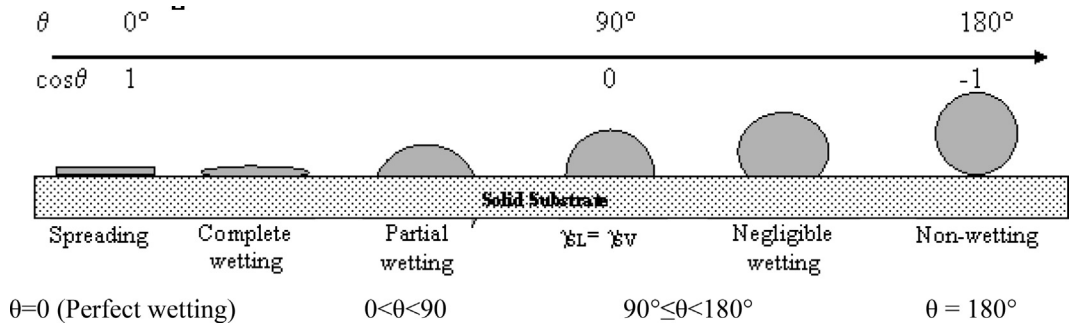

Fig. 1 Droplet behavior on a surface with different CAs [155].

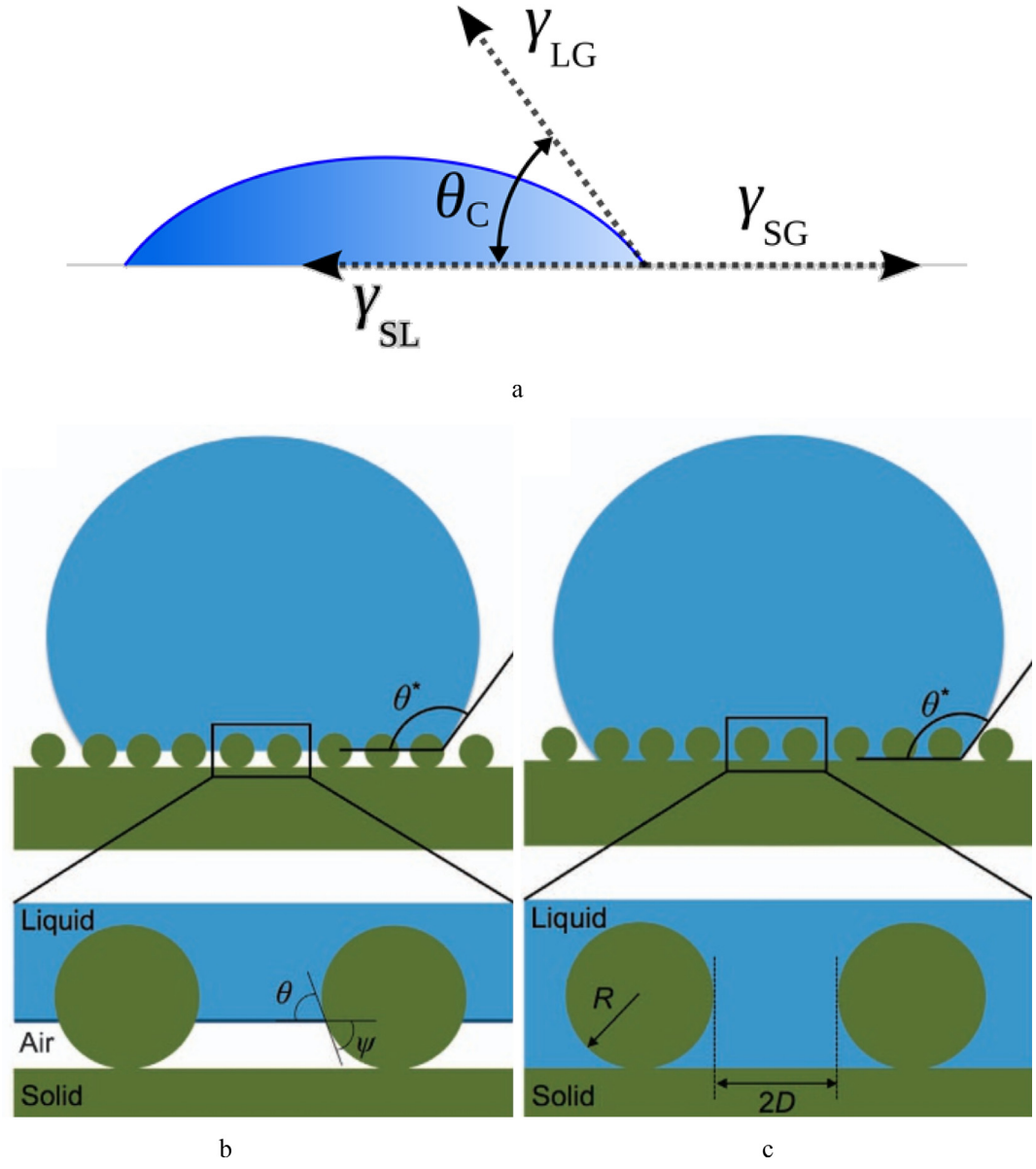

Fig. 2 Liquid drop schematic to depict the quantities in a- Young equation [6] b- Schematics of Wenzel state [156], and c- Cassie state [156].

Based on the Young–Dupré equation, the CA can be attributed to the adhesion work as [10]

$$\gamma_{LG}(1+\cos\theta_C) = \Delta W_{SLG} \tag{2}$$

where ΔW_{SLG} is the solid–liquid adhesion energy per unit area in medium G.

Young [11] was the first to specify the CA-surface tension relationship for sessile droplets on flat surfaces. A century later, Young's equation was modified, and the modified equation showed the dependence of the CA on droplet volume. The existence of line tension was suggested by Gibbs [12,13], and it acts on the three-phase interface and accounts for the surplus energy at the solid–liquid-gas phase interface; the CA e can be defined as

$$\cos\theta = \frac{\gamma_{SV}-\gamma_{SL}}{\gamma_{LV}} + \frac{\kappa}{\gamma_{LV}}\frac{1}{a} \tag{3}$$

where κ and a denote the line tension and the droplet radius, respectively. Although an affine relationship has been validated against experimental data between the inverse line radius and the cosine of the CA, it does not provide the correct sign of κ and it overestimates the value of κ.

On rough surfaces, a droplet could be in two different states. One possible state is the contact of a droplet with the entire rough surface, that is, the wetting of all the surface grooves under the drop [12]. In 1936, Wenzel established the principles of this mode (Wenzel mode) [12]. Wenzel stated that the actual liquid–solid contact area under a droplet on a rough surface is larger than that on a smooth surface. When the energy of the solid–liquid interface is lower than the solid-air interface energy, as the rough surface is wetted, more energy is withdrawn, and therefore the rough surface becomes wet faster. However, if the solid–liquid interface energy is higher, the

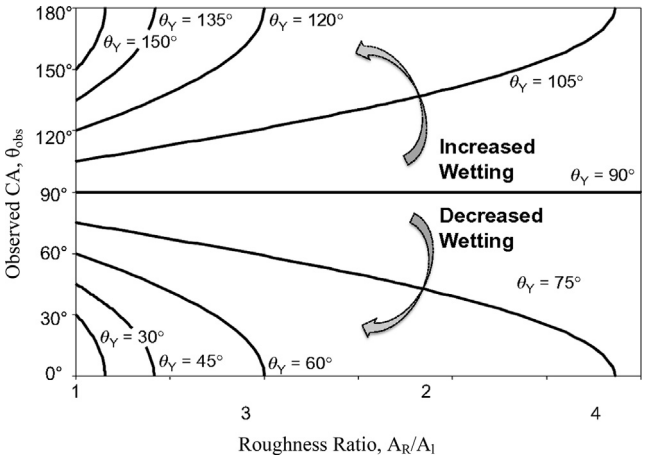

Fig. 3 Connection between observed CA and roughness ration based on Wenzel equation [16].

surface inherently repels water, and it becomes very difficult to wet the rough surface [14]. Wenzel corrected Young's equation to obtain Eq. (4) for the first time. The equation is known as Wenzel's equation and it shows that the CA increases by raising the CA of the rough surface:

$$\cos\theta_w = r\cos\theta_Y \tag{4}$$

where θ_w denotes the apparent CA in Wenzel's theory and θ_Y is the equilibrium CA of Young for the same substance on a smooth surface. Furthermore, r represents the roughness ratio of the surface and is given by Eq. (5). In other words, r is the ratio between the actual surface and the geometric surfaces [15].

$$r = \frac{A_r}{A_0} = \frac{\cos\theta_w}{\cos\theta_Y} \tag{5}$$

In this equation, A_r is the actual level, and A_0 is the observed level or geometric level.

According to the Wenzel equation, a drop tends to intensify the intrinsic behavior of the surface. In other words, if a smooth surface shows hydrophilic properties (i.e., $\theta < 90$), roughness further increases the surface hydrophilicity. Similarly, if a smooth surface exhibits hydrophobic properties (i.e., θ greater than 90), the roughness increases the surface hydrophobicity (see Fig. 3) [15]. The relationship between surface roughness and CA is shown in Fig. 3 [16].

However, the right side of the Wenzel equation may exceed one for specific surfaces, namely highly roughened surfaces or porous structures. In such cases, the Wenzel equation is invalid, and the Cassie–Baxter model is used instead [12].

The second feasible state for a droplet on a rough surface, shown in Fig. 2c, is that the droplet is suspended on surface protrusions and air is trapped between the surface protrusions under the droplets, known as the Cassie–Baxter mode. Cassie and Baxter developed an equation to determine the CA of a liquid on air–solid composite surfaces. At these coatings, air is trapped among surface grooves, which represents a main difference between Wenzel's theory and the Cassie–Baxter theory [15]. The Cassie–Baxter equation is defined as

$$Cos\theta_{cb} = 1 + f_{sl}(\cos\theta_Y - 1) \tag{6}$$

where f_{sl} is the fraction of the solid–liquid surface area, θ_Y is the CA of Young, and θ_{cb} is the CA of Cassie and Baxter. In this theory, the drop tends to exacerbate the inherent behavior of the surfaces stated earlier. The system in this model is more accurate than the one in the Wenzel model. However, it cannot be used to obtain a good idea of the parameters for surfaces where the roughness is distributed randomly. [15].

Fig. 4 compares the above-mentioned states for smooth and rough surfaces. A characteristic CA (θ) is formed by a droplet that rests on a solid surface and is surrounded by a gas. When there is roughness on the solid surface and the liquid is in close contact with the solid asperities, the Wenzel state is considered for the droplet. The liquid is in the Cassie–Baxter state when it rests on the asperities.

This theory is based on the influence of geometric factors on the surface upon the property of surface wetting. Equation (6), which is presented below, is referred to as the Bico and Quéré equation [17]:

$$\theta < \theta_c, \cos\theta_c = \frac{1-\varphi_s}{1-\varphi_c} \tag{7}$$

Here, θ_c is the critical CA, θ is the CA on a smooth surface with the same chemical composition as the rough surface, r is the roughness factor, and φ_s represents the volume fraction of the solid surface that remained dry. Thus, the following conclusions can be drawn:

For a flat surface ($r \to 1$), θ_c is equal to zero, which implies that flat surfaces become smoother if the CA (θ) reaches zero.

For porous surfaces ($r \to \infty$), we have $\theta_c = \pi/2$ (i.e., liquids with $\theta < \pi/2$), and the surface is wetted. In other words, the

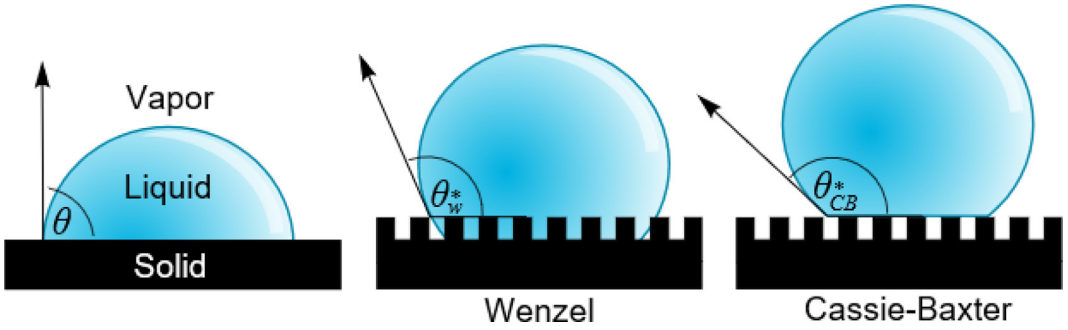

fig. 4 Schematic of water droplets on smooth and rough surfaces [157,158].

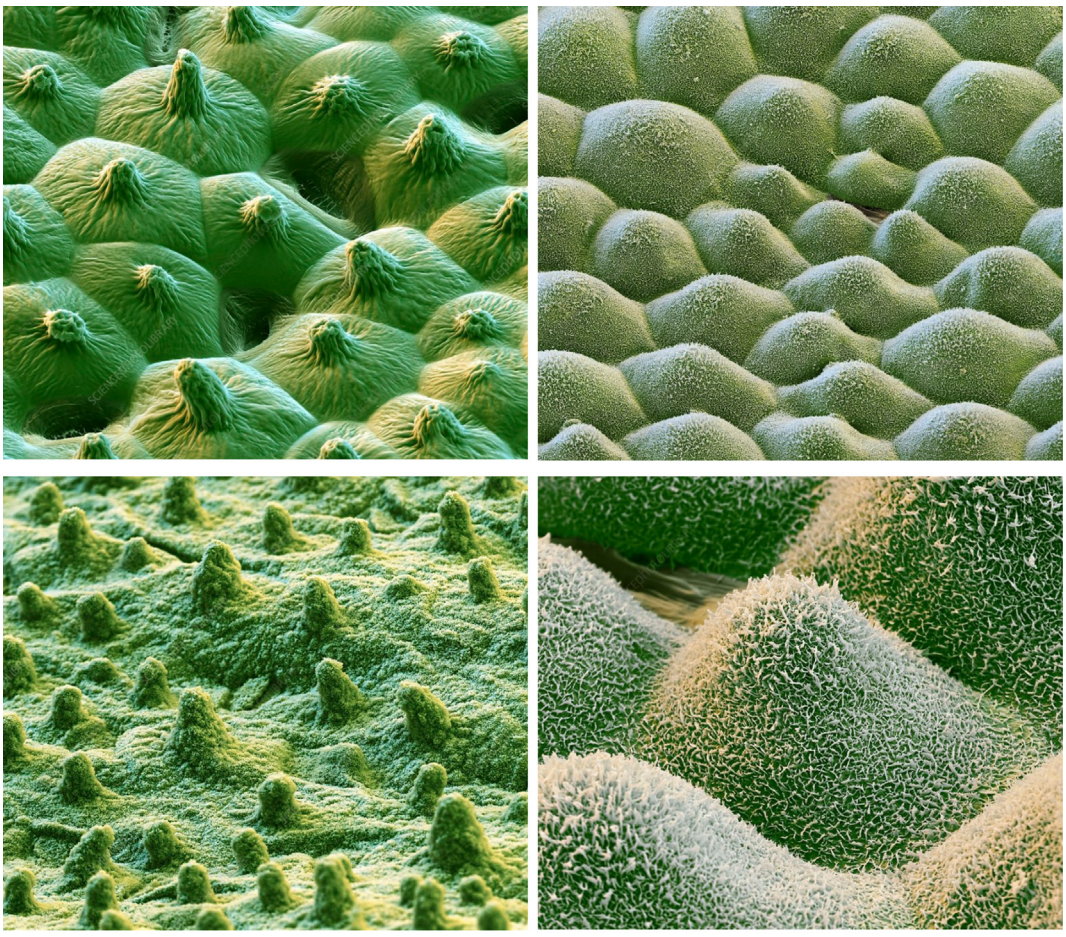

a b

Fig. 5 Microstructures on the top of (a) a lotus leaf (Nelumbo sp.) (b) a taro (Colocasia esculenta) leaf surface along with a waxy coating (removed here), help to increase hydrophobicity [159,160].

introduction of porosity increases the hydrophilicity of hydrophilic surfaces. Since φ_s and r are not always equal, the equation always gives a CA between 0° and 90° as the critical CA. Therefore, a porous surface with the capability to guide a liquid can be realized by appropriately designing the geometry of the surface [17].

Fig. 5a and 5b depict colored scanning electron microscopy (SEM) images of microstructures on a lotus leaf surface (*Nelumbo sp.*) and a taro leaf surface (*Colocasia esculenta*), along with a waxy coating. The excessive hydrophobicity of these leaves is attributable to the concurrent presence of double micro- and nanostructures and hydrophobic waxes on the leaf surface, which are abundant in soil plants [18]. An epidermal cell on the surface shows a micrometer-scale protrusion, which includes small, nanosized protrusions covered by a dense wax layer. The last layer of wax, which is 1–5 μm thick on the cuticle surface, is the main cause of the hydrophobicity. Similar hydrophobic properties can be seen in other plants [18]; nevertheless, the hydrophobic leaves of other plants have different surface structures. The hydrophobicity of these leaves is due to the crystalline waxes of the epithelial layer and papilloma skin cells [19]. Waxes are a mixture of aliphatic compounds, especially those without nonacosanol and nonacosanediol compounds [20]. One of the most typical features of these surfaces is their self-cleaning properties. Different particles, regardless of their size and chemical nature, are removed from hydrophobic leaves by natural or artificial rain. This continues until the complete removal of hydrophobic wax from the surface. However, some particles remain on the surface of the plants, which show high wettability, and they are removed only by heavy rainfall [19]. Fig. 6a and 6b show a reduction in the contact surface of droplets because of the unevenness of papilloma leaves and insect wings. In fact, the drops are in contact with only structure, which is located on the epithelial layer of the skin cells. Contaminant particles adhere to the liquid, as shown in Fig. 6b, and move with a drop on the leaf [19]. Decreasing the number of polar groups on the surface reduces the surface energy. This process is evident in most of the epithelial layer waxes, which are made of hydrocarbons. Here, a composite surface is formed since air is trapped between the grooves on the surface (Fig. 6c). The surface augments water–air interaction and decreases the water–solid contact. In this case, the droplets do not spread, and the water continues to be in the form of spherical droplets. The drop's CA is also dependent on the surface tension of water. On the other hand, because the particles are usually larger than the surface structures, they are in contact only with

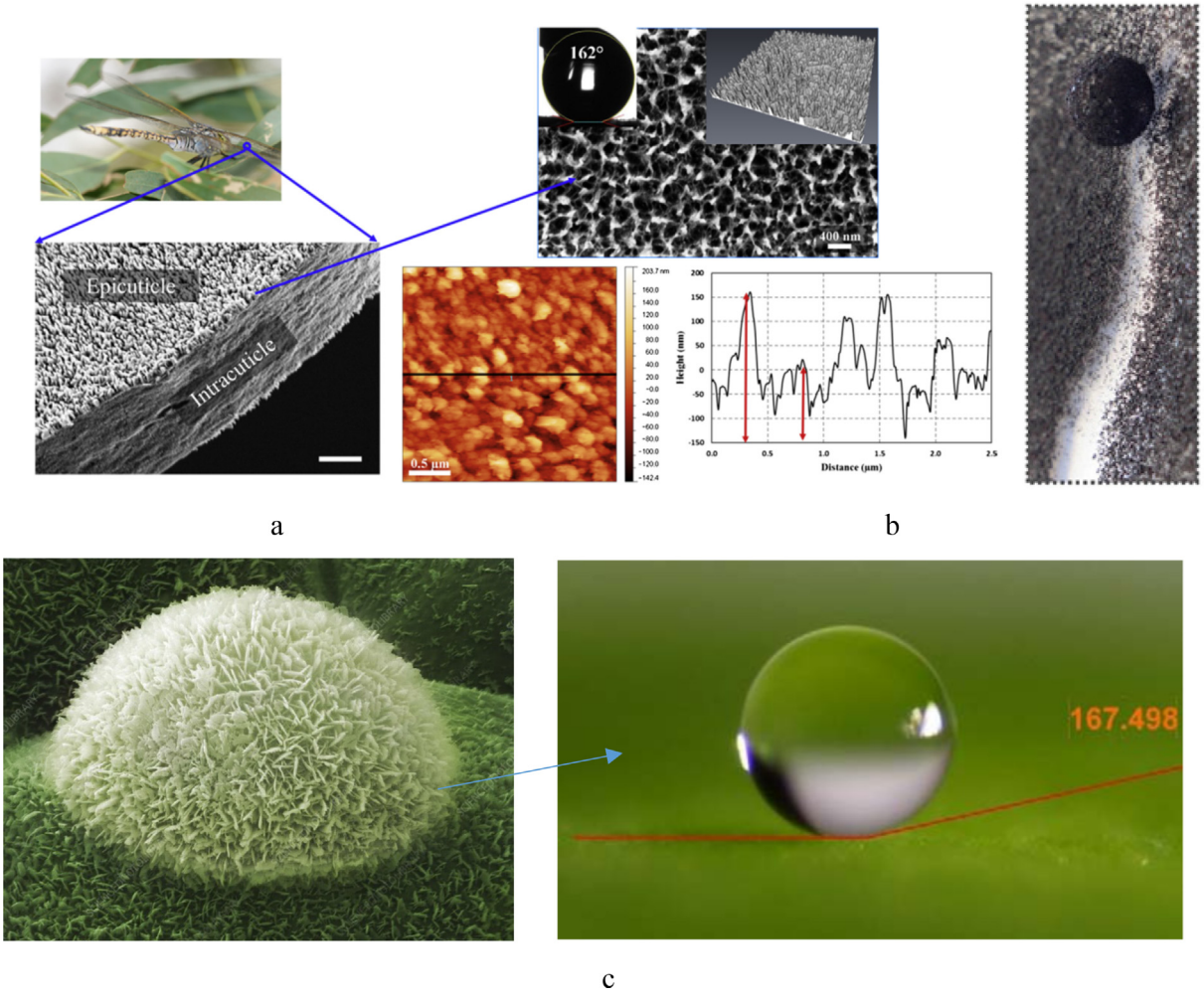

Fig. 6 A- wettability of the *Hemianax papuensis* dragonfly wing [161], b- Sticking contaminated particles to the droplet surfaces [162], and c- Effect of unevenness of the surface on the contact surface [163].

the uneven tip. Thus, the contact surface between particles and uneven tips decreases (Fig. 6a), and their tendency to stick to the surface of the water drop increases (Fig. 6b). Consequently, the droplet absorbs the particle to be removed from the leaf surface since there is no stronger force to overcome the adhesion of contaminated particles-water droplets.

Fig. 7 shows a schematic of the removal of contaminated particles from a smooth and uneven hydrophobic surface. Clearly, on a smooth surface with a small CA, the droplet velocity is relatively low. Therefore, particles attached to the droplet move together with the droplet; however, all particles are not removed. This is particularly the case for hydrophobic particles, and it is because of the surface energy between the particle and surface. Notably, hydrophobic surfaces with a suitable degree of roughness are effective in repelling contaminated particles. The self-cleaning mechanism (or lotus effect) is the most important property of these surfaces. In addition to plants' leaves, the bodies of light insects, such as butterflies and crickets, show SH properties. Furthermore, the feet of these aquatic insects are excellent examples of SH surfaces and keep the insects afloat. The wings of crickets or locusts have columns with a diameter of 80 nm and an interval of 90 nm, which makes them self-cleaning. The body surface of lizards, which has been the inspiration behind many innovations in nanotechnology, is an excellent example of a SH surface with self-cleaning properties [18].

In general, there are two approaches for fabricating hydrophobic surfaces and SH surfaces: 1) using materials with low surface energy to form a rough surface that is converted from a hydrophobic surface to a SH surface by changing the surface morphology and 2) modification of a rough surface by using materials with low surface energy. In the second approach, thin coated materials with low surface energy are deposited on rough surfaces. In practice, the two approaches are usually employed to manufacture hydrophobic surfaces and SH surfaces. Studies have shown that synthetic nanostructures mimicking the lotus leaf structure are suitable for creating SH surfaces [21]. The discoverer of the lotus effect, Wilhelm Barthlott, noted that the structure of the lotus leaf includes nanoparticles and microstructures containing a series of periodic arrays of hierarchical ridges [22]. Later, the development of high-precision SEM [23] led to more detailed studies of various microstructures on the plant's outer surfaces. Researchers have identified the nanoparticles and microstructures as the main causes of superhydrophobicity and self-cleaning properties. In other words, the nanostructures on

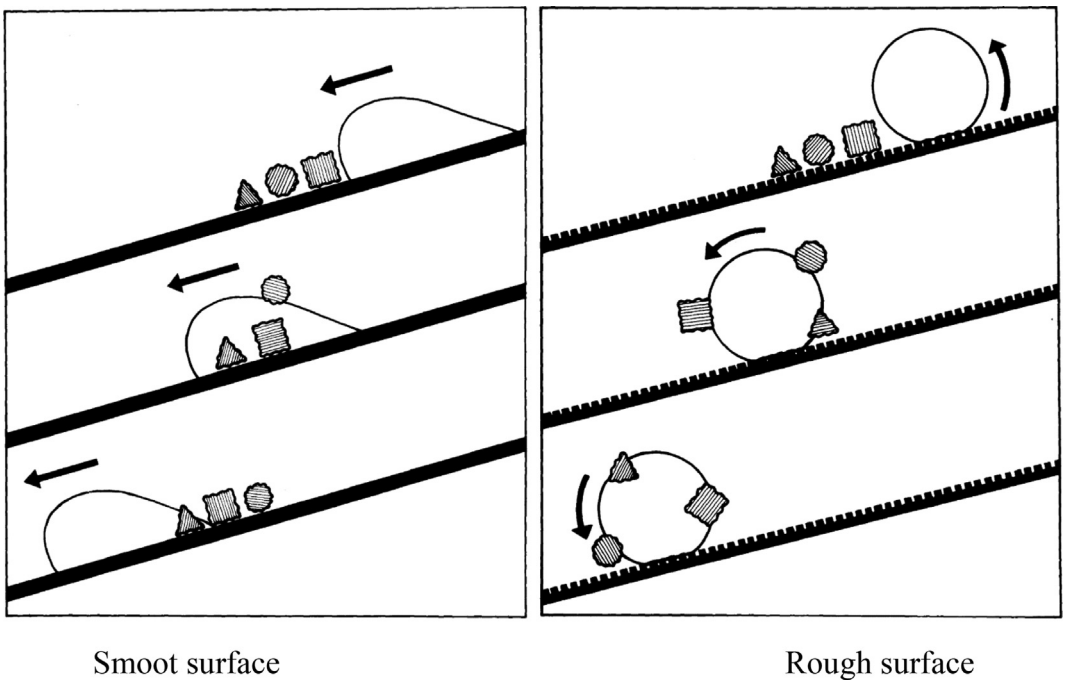

Fig. 7 Relation between roughening and self-cleaning [19].

the leaf surface of plants such as lotus give rise to air–liquid junctions on the surface. It is noteworthy that in the design of hydrophobic structures, in addition to controlling the surface energy of the coating, which is related to the type of material used, hydrophobic structures with SH properties are obtained by controlling the surface geometry. Therefore, structural parameters such as the shape and height of the ridges (effective height of the structured part) and the spacing between ridges are the main factors determining the self-cleaning rate of the structures [20].

Owing to their unique characteristics, hydrophobic surfaces can be used in various applications and industries, such as the textile industry (self-cleaning fabrics), the automotive and aerospace industries (self-cleaning glass, car bodies, and non-adhesive surfaces), the marine industry, optical devices and components (cameras, sensors, lenses, and telescopes), and in the construction of dams. One of the most important applications of these surfaces could be in the petrochemical industry. This is due to the fact that these surfaces are self-cleaning surfaces [24] with waterproof [25], anti-smudging [26], and anti-sticking [26] properties. They can hence be used for water harvesting [27], increasing heat transfer [28], in the energy field [29], for fabricating medical and electrical microstructures [30], for providing low-friction coatings and reducing drag force [31], for anti-icing [32], for anti-fogging [33], for smart fabric synthesis [34], for corrosion reduction [35], in solar energy panels [19], in anti-fouling coatings [36], in laboratory equipment and chips and heat transfer applications [37], and for separating oil from water [38]. Because of these features and applications of SH surfaces, SH coatings can help solve various natural problems and ultimately increase oil exploitation and reduce harvesting costs in petroleum industries.

At present, there is abundant information about hydrophobic surfaces and their use in various industries, but the use of these surfaces in the oil and gas industry is less mentioned. In this paper, to provide a profound understanding of the characteristics of SH surfaces, we first explain the angles related to the contact between a droplet and a surface, along with relevant essential theories. In the following, existing natural hydrophobic surfaces, artificial surfaces, hybrid surfaces, manufacturing methods for SH surfaces, manufacturing constraints, and the characteristics of SH surfaces that render the surfaces useful in the petrochemical industry are described in detail.

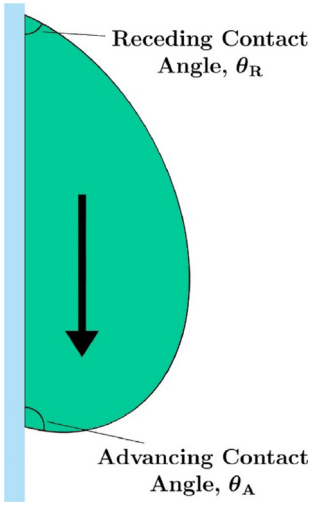

Fig. 8 Dynamic CA [164].

2. Wall contact angle

The wall CA (θ) of a liquid is measured by assuming that a drop of the liquid is placed on a flat, planar, rigid, and uniform

surface [39]. When a liquid drop is positioned on a solid surface, its non-diffusion results in the drop having a constant shape and equilibrium CA representing the solid surface wettability [40]. Geometrically, the CA is at the interface of the liquid–solid-gas phases [41]. According to Fig. 1, if the equilibrium CA is lower (higher) than 90°, the surface is hydrophilic (hydrophobic), while a surface with a CA exceeding 150° is regarded as a SH surface. Although obtaining the maximum angle of 180° is generally difficult [42], it has been achieved using advanced methods [43].

For many purposes, it is not enough to measure the CA of a stationary droplet, and measurement of other angles, such as dynamic CA [44], is recommended [5]. In this regard, a drop is assumed to be placed on a horizontal hydrophobic surface. A syringe slowly increases the drop volume until the liquid–solid interface shows no increase. This is called advancing CA, and the opposite case is termed receding CA (Fig. 8) [45]. In other words, to reach the equilibrium CA, the droplet should be subjected to equilibrium conditions over a sufficient time period. The static angles of advancing and receding contact are formed by increasing the droplet volume on the surface and then collecting the droplet from the surface. The advancing CA is typically larger than the posterior CA [46]. However, on SH surfaces, the two angles are very close, with only a slight difference. The angles formed behind and in front of the drop represent the dynamic receding (θ_R) and dynamic advancing CAs (θ_A), respectively, if the drop travels on an inclined surface, that is, if the drop moves on the boundary between solid, liquid, and gas phases. Different speeds may be used for measuring dynamic CAs. Dynamic CAs at measured low speeds should be approximately equal to static CAs.

3. Technological applications of SH surfaces

It is imperative for the petroleum industry to find ways to exploit renewable energy sources and increase the efficiency of oil recovery from existing reservoirs. The use of SH surfaces may aid in achieving this goal. Reducing ancillary costs is one way to increase efficiency in the oil and gas industry. Transportation networks, as indicated in Fig. 9, are responsible for some of these expenses. Using an appropriate passive method can prevent the corrosion of ships' hulls, masts, and pipelines and reduce drag force in the transportation network. In addition to the separation of water from oil, SH surfaces are very useful for other purposes in the petroleum industry, owing to the advantages that they offer. This section discusses some studies related to the technological applications of SH surfaces.

3.1. Corrosion-resistant surfaces

Corrosion is a major issue affecting the supply of oil and gas through pipelines [47]. Increasing resistance to corrosion has been one of the most important objectives in the industry for a very long time, and it has very significant economic consequences. In practice, corrosion damage cannot be totally prevented, but there are several techniques for slowing it down; examples are cathodic and anodic protection, and the use of protective coatings to slow down the rate of corrosion. In general, in a SH surface, it is expected that interaction between corrosive ions and the surface is prevented by an air barrier that exists between the surface and its corrosive surroundings [48]. Furthermore, since the extent of actual contact between the corrosive electrolyte and the surface is small, a SH surface has high resistance to corrosion to the electrolyte. Providing SH coatings on surfaces can protect them from external moisture and hinder electrochemical processes [49]. This has the potential to enhance the resistance to corrosion of the surface when exposed to very hostile environments. Thus, SH surfaces may be used to reduce the corrosion of metal substrates, including those made of magnesium and aluminum [50]. They can also be used to protect metal alloys, such as nickel and steel alloys. The anti-corrosion mechanisms of SH surfaces are discussed below.

Past studies have used many techniques for fabricating SH surfaces, and various methods have been used for their characterization and analysis. However, the conclusion of the studies has always been the same: SH coatings safeguard metallic substrates from corrosive environments. SH surfaces should have micro- and nanoroughness on their surface, and their surface energy should be reduced. The rough surface has large peaks separated by numerous valleys. Since SH coatings have an inhomogeneous structure, air can be easily trapped in the peak-to-valley pattern. Therefore, because of the trapped air, aggressive ion species such as Cl^- in electrolytes or corrosive conditions cannot easily corrode the underlying surface. In reality, the trapped air on the SH surface serves as a passivation layer, shielding the substrate from corrosive processes and thereby preventing its corrosion. It is quite easy for aggressive ions to corrode smooth metal surfaces that are exposed directly to corrosive species in their surrounding environment. The air trapped in the surface grooves of SH coatings may prevent corrosive substances from making direct contact with the material. Furthermore, the SH coatings would let more air get to the surface in the valleys, which would reduce the area of rough surface that is in contact with an aggressive solution. This is yet another major feature that explains why SH surfaces can increase the resistance to corrosion of metals, as demonstrated by Liu et al. [51]. The following equation can be used to compute the height (h) of the water column contained within the pipe:

$$h = \frac{2\gamma \cos\theta}{\rho g R} \tag{8}$$

where γ, ρ and R denote the surface tension, liquid density, and a cylindrical tube radius. The SH surface can be thought of as a vertical cylindrical tube that has been immersed in a liquid. The SH surface has a CA exceeding 150° and a much smaller pore diameter compared with other surfaces. Consequently, the Laplace pressure can drive a corrosive liquid out of the pores of the SH surface, allowing the substrate to be completely shielded from corrosion in the harsh environment in which it is used.

Recently, researchers have used SH coating without any toxic components to protect surfaces from corrosion. Such use of SH surfaces is possible due to the existence of air packets between the surface and the corrosive solution, which prevents the diffusion of corrosive ions and protects the substrate [52]. SH surfaces can reduce the rate of corrosion in metals by different orders of magnitude through hydrophobization. Many studies have shown the corrosion mitigation capability of SH surfaces. Using a commercially available hydrophobic

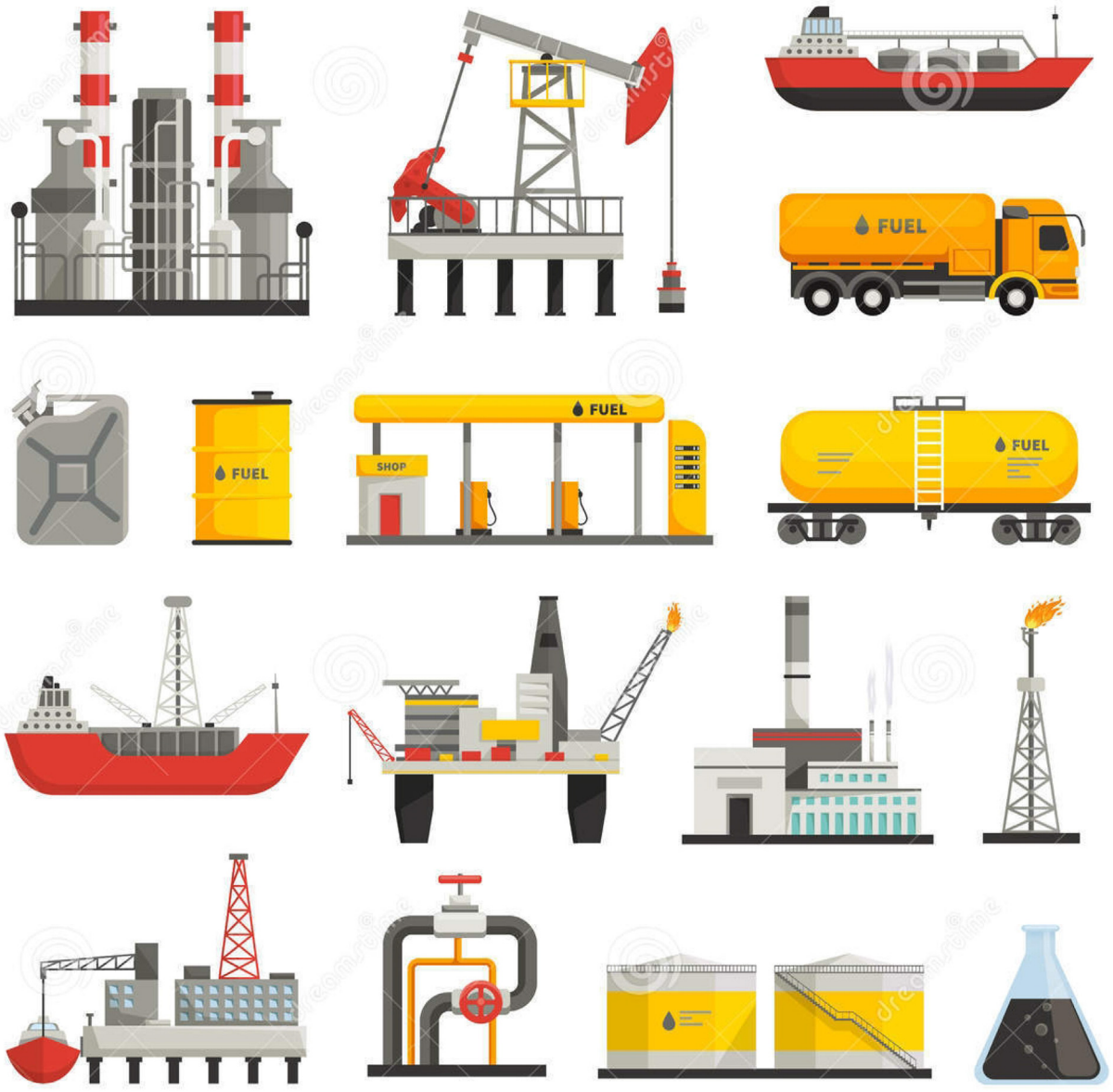

Fig. 9 Transportation networks in oil and gas industry [https://www.dreamstime.com/stock-illustration-oil-petrol-industry-icons-set-different-transports-constructions-factories-flat-isolated-vector-illustrations-image68304265].

coating treatment, the potentiodynamic polarization test showed that the corrosion current on metal surfaces was greatly reduced [53].

Fig. 10 shows the spreading factor of a water droplet that collided with SH (CA = 160°) and hydrophilic (CA = 80°) surfaces. Clearly, when the SH surface was used, the contact time and spreading factor of the droplet decreased dramatically. These two parameters are the main factors determining corrosion. Therefore, using SH surfaces is effective in reducing surface corrosion.

3.2. Oil and gas pipeline transportation and drag reduction

In the petroleum industries, drag reduction techniques for long-distance transportation pipelines have recently become a hot research topic. Pipeline transport involves considerable energy consumption because of the presence of frictional resistance against the fluid flow. Smoothing out the inner wall of the pipe has been a difficult task so far, but it could help. It is possible to lower the fluid resistance by providing a SH surface with decrease of drag capabilities on the inner layer of an oil transport pipeline, to reduce the overall energy consumption. In this case, a SH surface coating on a pipeline reduces drag by 14 % [54]. Moreover, the decrease of drag influence of a SH surface with secondary micro-/nanostructures is superior to that of a surface comprising primary structures. It has been experimentally demonstrated that a novel inner coating on a pipeline can significantly reduce drag compared with an uncoated pipe used as a control. The drag release efficiency showed a spectacular 8 % enhancement in comparison to the uncoated pipe [55]. Decrease of drag is of importance in the drilling and maintenance of pumping facilities in the petroleum

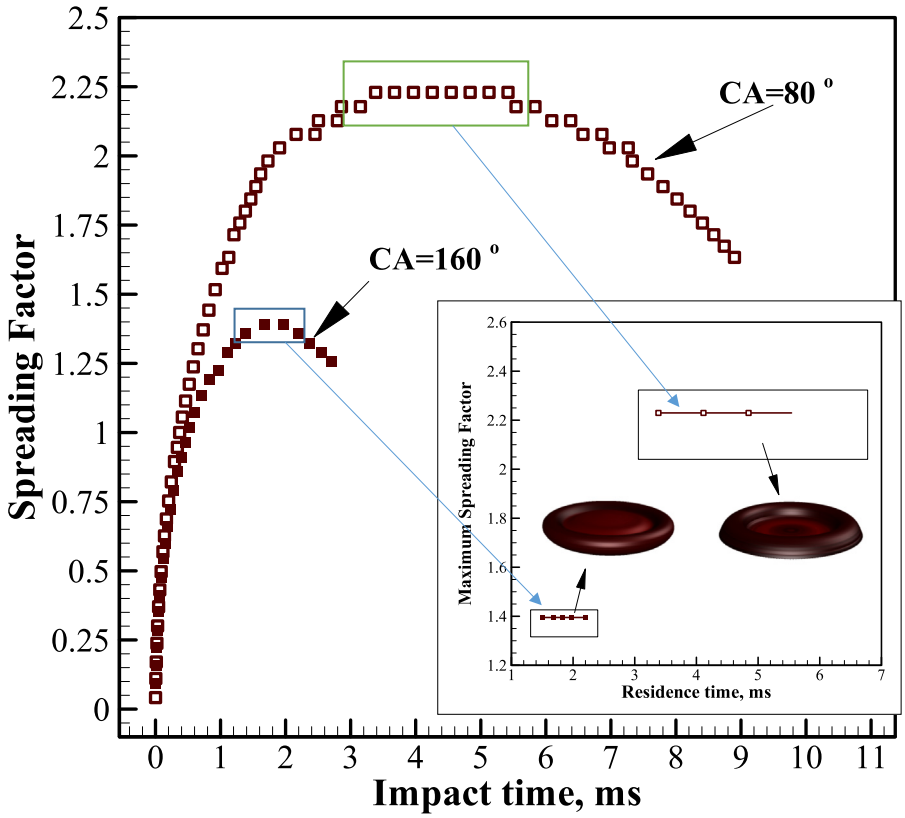

Fig. 10 Comparison of spreading factor and contact time of a droplet in collision with SH and hydrophilic surfaces [152].

Table 1 A summary of the existing investigations on using SH surfaces for drag reduction.

	CA, °	SA, °	Reduction in drag	Ref.
perfluorooctyltriethoxysilane	163	–	13	[171]
Mixture of stearic acid and lauric acid and FAS17	< 161	–	67	[172]
Perfluorotetradecanoic acid	160	3	20–30	[173]
biomimetic polydimethylsiloxane	151.74	–	19.2	[174]
perfluorooctyltriethoxysilane	163	2.7	31.6	[175]
N-dodecanethiol	159.7	–	38.5	[58]
commercial SH coating	165.8	–	20	[176]

industry. The addition of a small amount of high molecular polymer can result in the reduction of drag in pipes. Flow improvers, or drag reducing agents, have been in use in the petroleum industry for a long time. In the field of subsea production, piping typically presents a significant bottleneck because of the high cost of subsea installations [56]. Hydrodynamic drag force generated by the friction force between water and a moving solid surface in the water is a major issue faced in underwater motion. Inspired by shark skin, researchers have fabricated different SH coatings to decrease the drag force. As stated, SH coatings have air pockets inside their hierarchical micro-/nanoscale structures, which reduces the solid–liquid interface and thereby diminishes the drag. Decrease of drag by SH surfaces has been examined in many studies. A multifunctional TiO_2–SiO_2@polydimethylsiloxane hybrid material was proposed as a water-repellent ship coating owing to its low drag coefficient [57]. Another model was reported by Dong et al. [58]; by using electroless deposition of gold aggregates, they fabricated a SH coating on a model ship with a large and curved surface, and they achieved a 38.5 % decrease of drag due to the trapped air between ship and water (plastron effect). Decrease of drag has also been demonstrated through the contrast sailing test [59] and on a submarine model. Li et al. [60] showed that a layer of active air plastron with controllable pressure and superhydrophobicity helped achieve significant decrease of drag (92 %–96 % for high speed water jetting). Jeung and Yong [61] found that SH surfaces can decrease the drag force by up to 26.5 %. Overall, using SH surfaces is a solution for achieving pressure drops smaller than those occurring with untreated solvent at the same flow rate.

Fig. 11 An example of where atmospheric icing (frost, snow, rime, and glaze) and superstructure icing (sea spray icing) would be predicted to occur in different areas (A drilling platform such as the Eric Raude) [63].

Further information on the literature about applications of SH surfaces in decrease of drag is provided in Table 1.

The inset in Fig. 10 compares a droplet's form when it collided with SH and hydrophilic surfaces at a contact time of 0.65 s. Clearly, the SH surface led to a decrease in the wetted surface as a major factor contributing to drag enhancement. The reduction of the wetted area implied the reduction of motion resistant force. Thus, using a SH surface reduced the drag force dramatically.

3.3. anti-icing properties

Since the 1970 s, there has been a growth in offshore oil exploration and oil production in cold places such as the North Sea, Hibernia, Norway, and Alaska, and icing has begun to harm permanent infrastructure in these areas. Superstructure icing is a factor that can increase the complexity of a storm's impact and perhaps cause major damage [62]. Superstructure icing makes operations more difficult or requires activities to be paused or suspended until an icing event and its repercussions are managed. For example, increased offshore activities expose vessels, rigs, and workers to the risk of superstructure icing, according to the International Energy Agency. As a result of global warming, longer ice-free periods are expected, and they will be accompanied by longer fetches and, potentially, stronger polar lows that will occur farther north than they do today [63]. High winds that are frequent and long-lasting, along with prolonged fetch, result in higher wave heights and the possibility of more severe superstructure icing than that at present (Papineau, n.d.). Decks, for example, are particularly vulnerable to the formation of ice because of their horizontal orientation (Fig. 11). Vertical surfaces such as bulkheads, on the other hand, can become ice-coated when they become wet. A drill rig's height above the water line appears to be affected by ice [64]. Multiple forms of icing, including snow and sea spray, often occur simultaneously, especially in the wake of powerful winter storms. If ice loads are not removed after each event, they could have an additive effect on the vehicle's trim and stability [65]. According to reports, combined snow and sea spray icing caused a significant problem, which deserved additional investigation, off the Canadian East Coast [66].

Table 2 A summary of the existing investigations on using SH surfaces for anti-icing systems.

	CA, °	SA °	Ref.
graphene composite	155–165	3–7	[177]
polydimethylsiloxane	< 161	3	[178]
Micro/nanostructures and organosilane groups	159	–	[179]
polydimethylsiloxane	155	5	[180]
Micro-cubic array structures	149.61	< 8	[181]
concrete coating	160 ± 1	6.5 ± 0.5	[182]

The conventional approach to anti-icing is primarily based on a melting method that requires significant energy, but it is not completely successful [67]. Several biomimetic anti-icing mechanisms have been identified in recent years, including anti-icing (preventing droplets from sticking to the surface and removing them directly before they freeze) [68], Suppression of ice nucleation (postpone the crystallization of droplets of water, which makes freezing take longer) [69], and removal of ice (reduction of adhesion force between the ice and the surface thereby allowing the ice to easily fall off) [70]. Recently, SH coating has been used as an anti-icing coatings. As mentioned, the existence of air packets on SH surfaces helps droplets slide easily on its surface. Consequently, the residence time for freezing the droplet will not be sufficient, which reduces the frost's side effects on surfaces. Obviously, ice storms are one of the most important phenomena causing

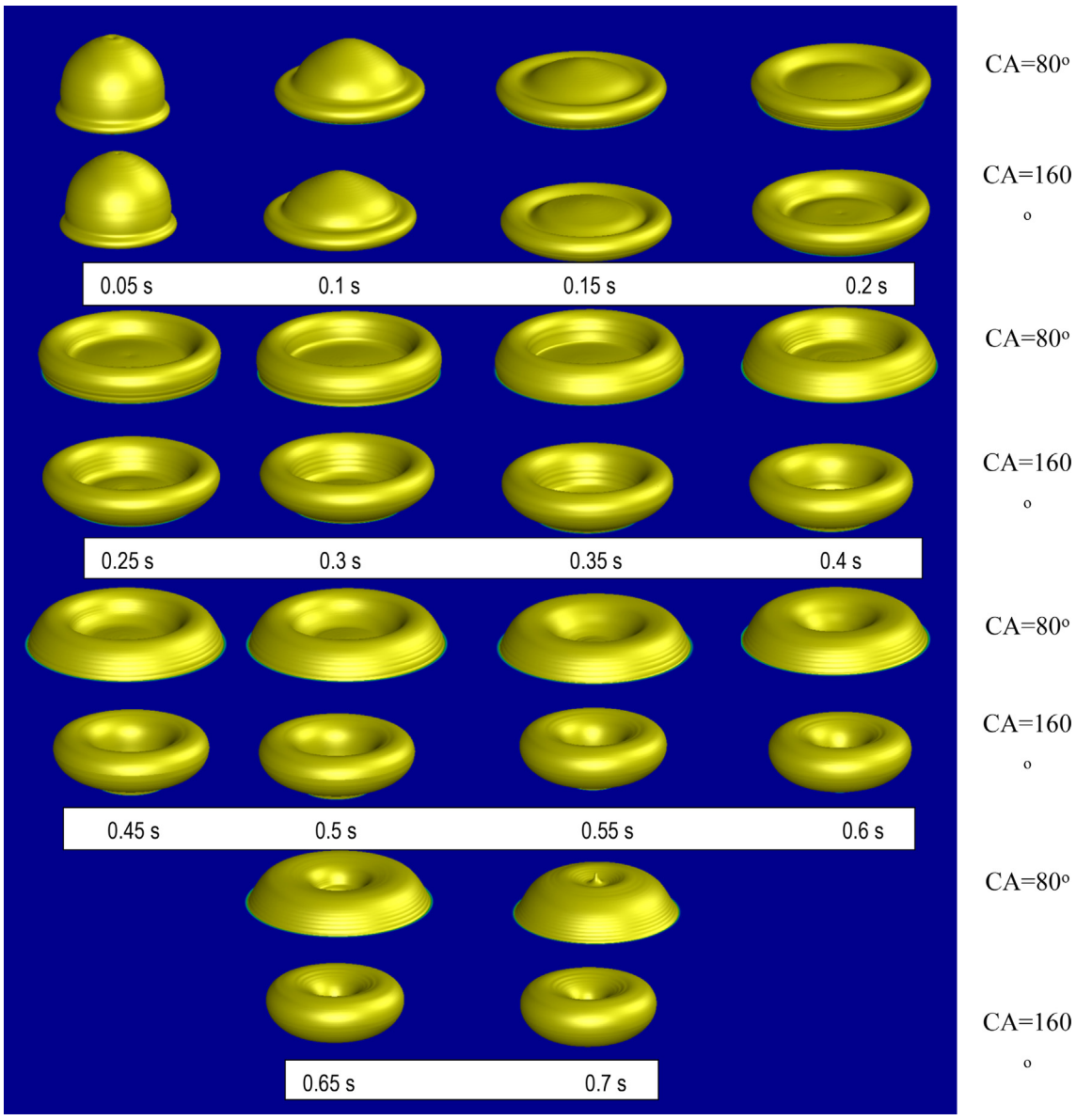

Fig. 12 Droplet behavior in collision with a surface with various CA [165,166].

damage to sensitive electrical equipment and aerospace facilities. The unique characteristics of SH surfaces could be used in most cases to reduce such damage. Experimental investigations have shown that using SH coatings can protect equipment from icing, even up to −5°C, and saturated humidity have indicated that SH surfaces are useful for decrease of ice adhesion to the surface by up to 97 % [71]. Some investigations on the use of SH surfaces in anti-icing systems are listed in Table 2. Fig. 12 visually compares the deformations of a droplet in collision with hydrophilic and SH surfaces. Evidently, after the impact time of 0.15 s, the SH surface led to a reduction in the wetted area. Since reducing the contact surface reduces heat transfer, when a droplet collides with a cold surface, there is little time for heat transfer from the droplet to the surface. Thus, the use of a SH surface reduces the icing process of a droplet on the surface at low temperatures.

3.4. Self-cleaning surface

Inspired by the photosynthesis process of the green leaves of trees, researchers have developed hydrophilic surfaces that destroy the chemical structure of pollutants in the presence of sunlight through photocatalysis processes [72]. One of the materials that can be used as an self-cleaning surface is titanium dioxide [39]. In 2001, Pilkington Glass was introduced as the first commercial self-cleaning coating comprising thin transparent layers of titanium dioxide [40]. Titanium dioxide cleans glass through two mechanisms, namely photocatalysis and hydrophilicity. During the photocatalysis process, the chemical structures of organic contaminants and other impurities on the coating are broken down by the absorption of sunlight. The hydrophilicity of the surface reduces the wall CA, creating a water film on the surface that removes contaminants. Under normal conditions, titanium dioxide absorbs

light with an energy higher than its energy gap [73]; therefore, charge carriers are generated. Negatively charged electrons (-e) and positively charged (+h) holes cause a few charge carriers to migrate to the surface. Cavities oxidize organic molecules on the surface while atmospheric oxygen is combined with electrons to form superoxide radicals. At room temperature, these radicals strike nearby organic molecules, which turns the pollutants into carbon dioxide and water [41].

It is noteworthy that titanium oxide is not very active in the visible region and can only absorb 4 % of the visible sunlight [74]. This compound usually exhibits ultra-hydrophilicity properties under ultraviolet light [75]. Through the addition of metals such as chromium, manganese, cobalt, and iron to titanium dioxide nanoparticles, they can be made to perform photocatalytic degradation of pigments under visible light [42]. When titanium oxide polycrystals are deposited with cobalt, the energy gap in titanium oxide decreases because of the interaction of cobalt ions in the titanium oxide network and the formation of new bonds [73]. The electrons in the crystal lattice can then be transferred to the conduction band through light absorption in the visible region. Thus, photocatalytic activity in titanium oxide can be performed, and adding chromium to the structure of titanium oxide reduces the light absorption edge and increase absorption in the visible region [43]. The ultra-hydrophilicity of titanium dioxide is also induced by sunlight. The cavities formed by optical excitation in titanium dioxide collect oxygen from the surface of the electron material and oxidize it [76]. Therefore, free oxygen radicals are formed on the surface, which allows hydrogen bonding. Bonding between oxygen and hydrogen radicals results in hydroxide groups being formed on the surface, leading to smaller CAs [41]. The photocatalytic activity of titanium dioxide increases when it is used as a thin layer of nanocrystals. Aside from titanium oxide, other materials like WO3, CdS, ZnO, and ZrO2 can also be used to make surfaces that clean themselves. The properties of a material's surface are often different from those inside the material [77]. This is because the atoms and molecules adjacent to the surface of the material are less bonded to atoms inside the material and hence are thermodynamically more unstable. This instability manifests itself in the form of higher free energy [77]. Besides, energy levels at the surface are discrete; these levels are compressed within the material and create an energy band structure [78]. At the nanoscale, the surface-to-volume ratio is considerably high, and the possibility of occurrence of surface cavities and the chemical decomposition of contaminants increases. Hence, titanium oxide nanoparticles are commonly used as ultra-hydrophilic surfaces [79]. In contrast to hydrophilic surfaces, hydrophobic surfaces prevent water from spreading or being absorbed on the surface; they cause water to drip and slip because of their micrometer- and nanometer-scale surface roughness. hydrophobic surfaces have shallow surface energy, while the hydrophilic surface energy is significant [8]. The use of nanotechnology and the emergence of different properties at nanometer dimensions have resulted in the realization of SH and ultra-hydrophilic surfaces.

3.5. Solar cells

Solar photovoltaic (PV) technology, being both efficient and clean, is becoming more and more important in the petroleum industry. According to reports [80], around 10 % of the oil produced in 2013 was used for oil production and processing, and a considerable part of the energy used was used for heating in the oil processing industry. Solar energy can be used in oil production and processing, and such use can save a significant amount of oil and gas and reduce the emission of greenhouse gases [80]. Thus, solar energy development and utilization for oil production in oil-rich regions are feasible in most cases [81]. The many applications of solar energy in the oil industry include the generation of heat and electricity, the treatment of water produced by oil wells, and the refinement of crude oil [82]. To date, solar energy has been employed extensively in oilfields for the three aforementioned purposes, and research has been performed to determine whether solar energy can be used for refining oil. The current focus is on how to use solar energy to achieve high-temperature catalyst conditions, and this subject is now under investigation. Over the course of four decades, perceptions about solar energy among oil giants have changed constantly and dramatically. As a result of the current restrictions on greenhouse gas emissions, big oil companies are more likely to speed up the development of solar energy.

An anti-reflection layer is introduced on the outside of a photovoltaic solar cell to allow photons to enter [83] for absorption by the cell. Heavy oil exploitation and high levels of solar radiation are required in some locations around the world. However, the performance of solar PV modules used to make electricity is affected by things like the amount of sunlight, the speed and direction of the wind, the temperature, the humidity, and the amount of dust in the air [84]. Hence, producing solar panels that are resistant to pollution over a long period of time is critical to maintaining the long-term and efficient operation of solar cells [85,86]. Antireflective surfaces with SH qualities are getting a lot of attention right now because they could be used to solve important technological problems. In addition to their unique surface texture and chemistry, which govern their wettability, SH surfaces have self-cleaning qualities as a result of their high wettability. Surface micro-/nanotexturing, in combination with reduced surface energy of materials, results in improved anti-wetting capabilities of materials [87]. Because the CA on self-cleaning surfaces is greater than 150°, the surfaces display exceptional anti-wetting qualities, resulting in the rapid roll-off of water droplets upon contact. The same is true for transparent coating materials that change the optical path in the right way, which could reduce surface reflection. Transparency is a key part of enhancing the effectiveness of optical devices like windows, lenses, solar panels, and even in other applications [88]. Typically, a solar panel is only able to collect around 25 % of the solar energy that strikes it; the rest of the radiation is simply reflected back into space. The development and use of transparent SH surfaces that reject atmospheric dust on solar panels and the resulting reduction in the reflectivity of the solar panel surfaces is very desirable [87].

Most offshore rigs are mainly powered by hydrocarbon energy sources, which leads to high levels of ecological footprints. These effects can be reduced by using solar power for sustainable petroleum exploration and production. In view of the self-cleaning of SH surfaces, self-cleaning micro-shell structures with SH surface behavior were employed in a solar cell. It was observed that such a structure prevented degradation by dust particles and thereby enhanced the efficiency of solar cells [89]. An additional study demonstrated that a super-

hydrophilic nanopatterned glass surface that did not have any surface chemical treatment had effective self-cleaning and antireflective properties with just a 1.39 % loss in the efficiency of the solar cell. However, bare glass packaging and packaging of fluorinated SH resulted in a 7.79 % and 2.62 % drop in the solar cell efficiency, respectively [90]. Furthermore, a TiO_2-coated mesh film with micro- and nanostructures has been used for the oil/water separation [91], and a SH polymer-coated copper mesh has been used for the separation of organic solvents from water [92]. Additionally, a strategy has been proposed for the fabrication of robust self-cleaning SH surfaces, which can be used on soft and hard substrates. This strategy results in a surface with remarkable robustness against knife scratches and sandpaper abrasion [93]. Table 3 provides a list of studies related to the use of SH surfaces in solar photovoltaic systems.

3.6. Heat transfer

Consistent and reliable thermal management is of high importance to the petroleum industry. Thermal management in oil and gas processing is often difficult because of the large number of pieces of equipment used and their complexities [94]. Condensation occurs in heat exchangers that are employed in thermal applications like air conditioning, collecting water, getting energy from the sun, and getting salt out of the water. The energy consumption for these thermal applications has already sparked widespread concern about the availability of energy and the potential environmental consequences. Furthermore, the thermal efficiency of heat exchangers has a direct impact on the overall efficiency of the entire petroleum system. Hence, improving the heat transfer performance of thermal applications could help save considerable energy [95]. In this regard, it has been found that the use of SH surfaces significantly improves a heat exchanger's performance.

In some parts of the world that are oil-rich, temperatures sometimes drop to −35 °C. The extremely low temperature can gelatinize crude oil [96]. In such areas, the heat transfer process is very important. Many investigations have focused on the heat transfer properties of SH surfaces, especially for oil–water separation. A new mode of condensate sinkage was proposed for roughness-induced SH surfaces to explain the non-condensable gas influence on the condensation heat transfer efficiency of a steam–air mixture [97]. The condensation performance and convective condensation heat transfer of finned tubes with hybrid wettabilities (hydrophilic-SH hybrid) have also been studied in the presence of large amounts of non-condensable gas [98,99]. In order to increase the condensation of droplets on SH surfaces, one study created patterns on SH aluminum surfaces by using carbon dioxide laser-processing techniques [100]. In another study, stable dropwise condensation was found to occur on a bioinspired hydrophilic slippery surface with non-condensable gas. The condensation also increased the heat transfer rate, showing its potential for use for a low degree of subcooling or a large non-condensable gas concentration [101]. Another investigation conducted into the effects of steam condensation heat transfer on a honeycomb-like microporous SH surface demonstrated that condensation heat transfer increased various non-condensable gas concentrations on the SH surface throughout a broad range of subcooling, up to about 35 K [102]. Besides self-cleaning, SH surface can also be used for energy storage in wet and humid environments [103]. SH surfaces have also been employed for medical applications. A SH material based on fluorinated alkyl side-grouped poly (carbonate urethane) containing carbon nanotubes was created; it exhibited outstanding platelet antiadhesion and blood compatibility [104]. It has also been demonstrated that SH surfaces with only nanoscale roughness reduce adhesion and proliferation of 4 T1 mouse mammary tumor cells compared with SH surfaces with microscale structure [105].

Table 3 A summary of the existing studies on using SH surfaces for solar systems.

	CA, °	SA °	Ref.
3D crosslinked network of nanopores and silica nanoparticles	157.9	1.2	[183]
Hybridizing ZnO Nanowires with Micropyramid Silicon Wafers	171.2 ± 1.8	1.9	[184]
Nanograss films using glancing-angle deposition of an electron-beam evaporated source material on glass	greater than150	–	[185]
aluminium oxide coatings	155		[186]
silica nanoparticles	146	< 10	[187]
metal layer on a silicon surface	greater than150	1.5	[188]
polyethylene terephthalate	160	13	[189]
ZnO based micro-/nano-hierarchical	162	greater than2	[190]
three-dimensional micro-pillar arrays on the ethylene-tetrafluoro-ethylene films	155	15	[191]

3.7. Water collection

In deep oilfield drilling, a number of issues, including poor driving of water and major conflicts between planes, layers, and interlayers, are encountered [106]. Water collection with SH surfaces is another application of SH surfaces. For such an application, SH surface-modified cotton substrates with *n*-dodecanethiol and gold micro/nanostructures are used. Such modification leads to the fabrication of SH surfaces with a CA of greater than 150 [107]. Zimmermann et al. [108] manufactured the SH textile fabrics. However, since the traditional CA is not suitable for obtaining SH textile properties, the water shedding angle was defined for this purpose [108]. This value specifies the minimal angle of inclination at which a droplet entirely leaves a surface. Superhydrophilic star-shaped patterns for a titanium dioxide (TiO_2) SH surface, a titanium dioxide-copper (TiO_2-Cu) composite surface modified with thiol [109], a hybrid superwettable coating surface with superhydrophilic nanoparticles [110], SH coating [111], and a surface with a well-ordered hierarchical nanoneedle structure [112] have been found to show excellent water collection. Wang et al. [113] demonstrated that an increase in a nanostructure's height or a decrease in a nanostructure's diameter resulted in a reduction in the defrosting temperature. Thus, to save energy in the defrosting process, the nanostructure size of the surface should be optimized. Such a structure also helps

small water drops converge into large drops and makes them roll off the surface before freezing, which results in the surface showing anti-icing property. An acrylic polymer-silica nanoparticle composite on a glass substrate [68] or stainless steel [114] also has anti-icing property. Farhadi et al. [115] noted that in a humid atmosphere, the anti-icing efficiency of SH surfaces is reduced because of water condensation, which is the main limitation of such surfaces.

4. Creation of SH SURFACEs

In general, skin microstructures of tree leaves can be divided into two categories: hierarchical microstructures (Fig. 13a,b) and unitary microstructures (Fig. 13c,d) [117].

The findings discussed in the previous show that synthetic SH surfaces mimic natural leaf surfaces. So far, many researchers have attempted to produce modified surfaces [118–120] and surfaces that have very low surface energy and to control the surface morphology on the micro-/nanoscale, for realizing a hydrophobic surface [121,122]. Researches have shown that making CAs greater than 120° on a flat surface only by manipulating the water-repellent chemical structure of the surface without introducing nanoscale or micro-textures is almost impossible. Therefore, there should be two surface roughness components and an aqueous chemical structure (low surface energy) to form SH surfaces [123]. The surface roughness can be expressed using the Wenzel equation, which predicts that if the molecular level of hydrophobicity is rough, it will show high hydrophobicity [124]. Broadly, there are several methods to design SH materials, including dip-coating [125], a sol–gel method [126,127], a hydrothermal method [128], electrospinning [129], etching [130], anodization [131], electrodeposition [132], laser treatments [133], lithography [134], a template method [135], a layer-by-layer method [136], and modification of natural fibers [137]. The rapid increase in SH surface applications has led to increased interest in the development of fabrication methods for these surfaces. Table 4 shows some recent methods for the manufacture of SH surfaces with their CA and sliding angle (SA).

By oxidizing a sample surface and then changing it with a single layer of *n*-octadecyl thiol, a surface made of SH zinc oxide was made with high durability [138]. This procedure is amongst the simplest SH surface fabrication methods [139]. Qing et al. [140] demonstrated that spraying SH coating over a sandpapered surface resulted in a SH sample with excellent anti-icing property. For the first time, Pei et al. [141] fabricated a hydrophilic-hydrophobic reversal surface. The manufacturing procedure included UV-induced thiolene interfacial click reaction of thiol-modified palygorskite nanorods (Pal-SH) with polydimethylsiloxane diacrylate. Wang et al. [142] compared the spraying method with the wet chemical etching method for SH surface fabrication and demonstrated that the former is more efficient than the latter. However, the frosting problem should be resolved before applying the sprayable SH coating.

5. Restrictions on coatings and SH surfaces

Recently, researchers have presented numerous reports on the exciting and unique behavior of SH surfaces and materials. However, so far, none of the SH surfaces has been commercialized. The most important reasons are listed below.

a. Costs: With the exception of SH diatomaceous earth, the materials that are SH are costly. This is because of the significant amount of processing required to produce

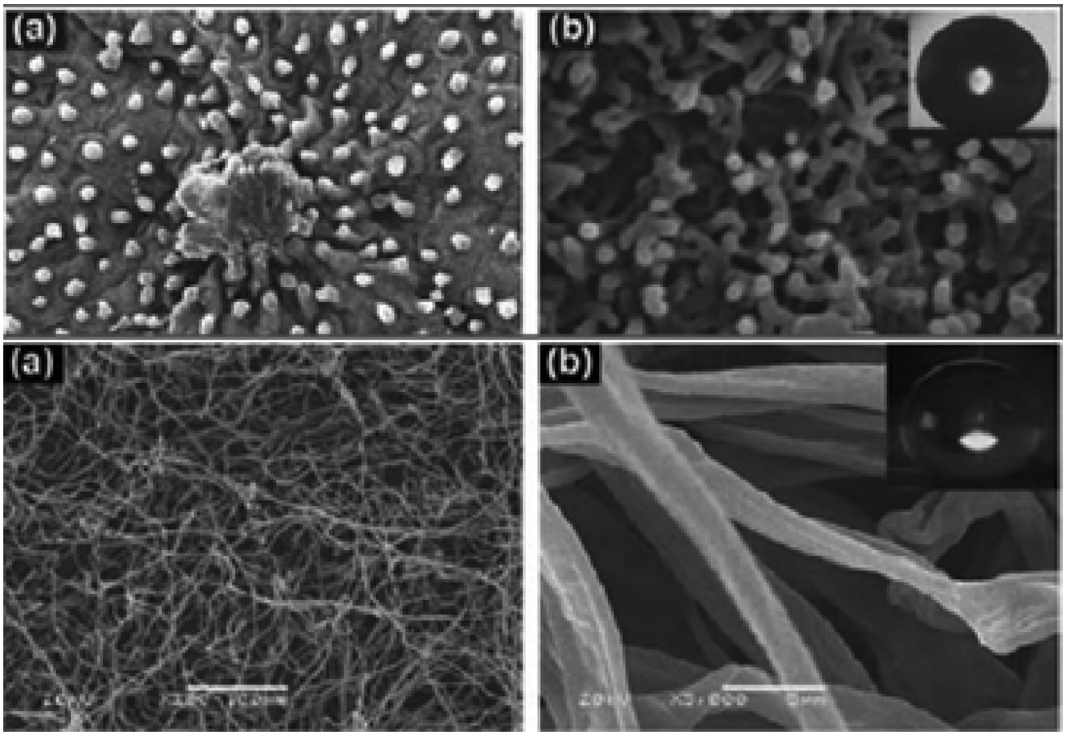

Fig. 13 A-b) Hierarchical microstructures and c-d) Unitary microstructures [117].

Table 4 Some recent methods to create the SH surfaces.

Ref.	CA°	SA°	method	Application
Zhang et al. [192]	156	5	combines droplet etching and chemical modification	thermostability, anticorrosion, self-cleaning and antifouling
Mahadik et al. [193]	163 ± 2	5 ± 1	sol–gel spray coating	long-term industrial and domestic applications
Wang et al. [194]	152 and 145	15 ± 1 and 23 ± 2	Roll-to-roll melt hot-pressing	self-cleaning, packaging and drag reduction
Liu et al. [116]	162 ± 5	4	Solution immersion process	cohesion strength and high- and low-temperature resistance
Ma et al. [195]	156	–	Thermoplastic forming	mechanical stability and resistance to corrosion
Wang et al. [138]	154	2	electrodeposition	excellent anti-corrosion effect and self-cleaning
Ji et al. [196]	162	2	Grinding and acid etching	repellency of the low surface tension liquid, hexadecane, and the rolling behavior
Liu et al. [197]	163	~ 1	calcination process	Transparent, durable and thermally stable
Sun et al. [198]	158.6 ± 1.3°	1	chemical etching	anti-icing ability, thermostability, and mechanical durability
Lv et al. [199]	150	10	Sanding and etching	UV resistance, and thermal and mechanical stability.
Barthwal et al. [200]	156	4	sol–gel	Self-cleaning, oil–water separation, and flame retardant
Pan et al. [201]	161 ± 2.5	~8	picosecond laser texturing	Antibacterial Adhesion
Zhang et al. [202]	158 ± 2	5	simple dip-coating	Self-cleaning
Sriram et al. [203]	170 ± 2	8 ± 1	solution-casting	Separation of oil–water
Seo et al. [120]	~ 99.82°	–	single-electrode mode Triboelectric nanogenerator with cilia microstructures	Energy Harvesting

the micro-/nanostructures of these types of surfaces. For example, most nanosurfaces and SH microstructures have recently been developed by the photovoltaic process [143], which is an expensive process. Notably, photolithography is done on a small chip, and the total cost of this method for large surfaces is prohibitive.

b. Performance of nanostructure: A high-quality SH surface requires water-repellent surface chemistry with constant topography on micro-/nanoscales. Achieving this with a simple set of requirements is not possible. This is because the nanotextured polymers easily bond together and quickly lose their hyperactivity [144,145].
c. Durability: Even if high-quality SH particles are used, these particles cannot be easily attached to the substrate without a significant reduction in their superhydrophobicity behavior. This condition tends to involve a compromise between two desirable but incompatible characteristics, namely durability and superhydrophobicity behavior [146].
d. Densification: Although repelling water is the main feature of SH coatings and surfaces, they cannot repel water vapor. Hence, precipitation and condensation cause a considerable extent of surface wetting [147].
e. Impact: The trapped air layer associated with SH surfaces is destroyed or decreased by the local high pressure of water. It is because of local water flow or slight and easy abrasion of the surface during immersion in water. Since superhydrophobicity is a surface characteristic, any significant surface impact causes local defects in superhydrophobicity behavior [148].
f. Wettability of activating agents: Increasing the water surface tension leads to superhydrophobicity behavior. Conversely, superhydrophobicity is greatly reduced or eliminated by reduction of the water surface tension by using surface activating agents or oils [149].

6. Natural superhydrophilic-SH hybrid surfaces

A hybrid surface [150–152] is a new type of surface that has been considered for various applications in recent years. Plants such as *Alchemilla mollis* and *Euphorbia* have SH leaves, and the central parts of these plants are highly hydrophilic. This is because of the various structures and chemistries of these surfaces and the possibility of water accumulation because of the presence of SH areas with a high adhesive state; an example of this is found on the surface of the red rose. When the droplet reaches a certain size, the leaves of this plant twist, and water droplets are directed toward the plant's stem. A similar mechanism has been observed in Namib Desert beetles. With this process, this insect can absorb morning fog and survive in very hot environments. Researchers have shown that

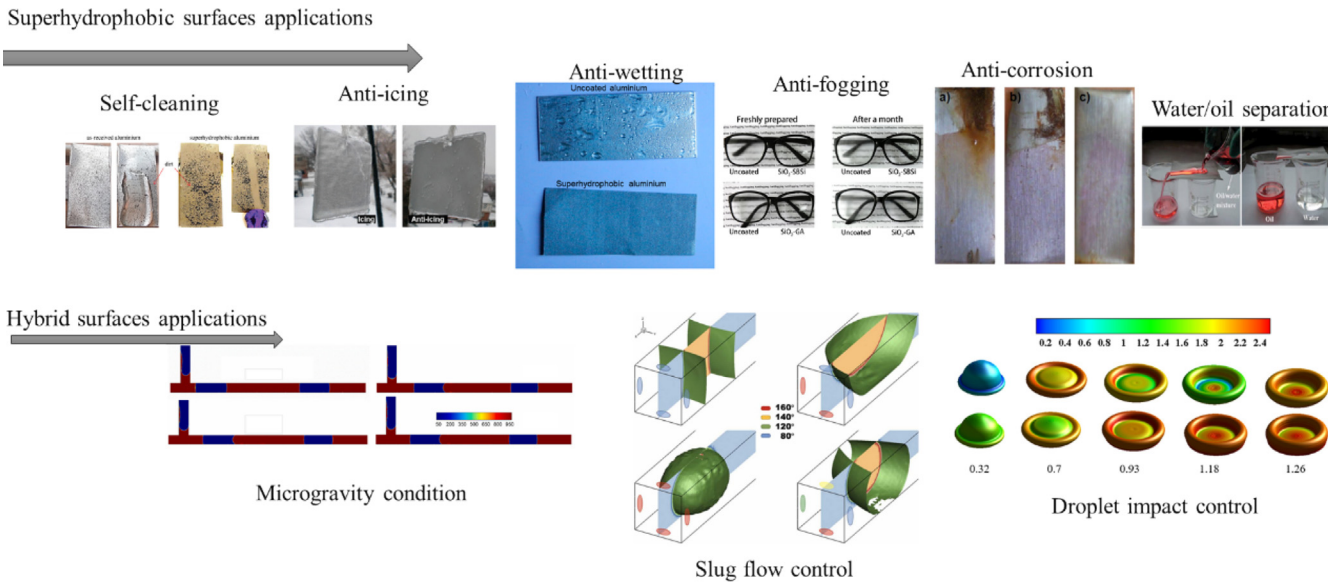

Fig. 14 Path of using surfaces with various ca patterns [68,150–152,167–170].

this ability is due to the existence of a SH waxy coating, covered with areas of hydrophilicity. When the water droplets are large enough, these areas direct the droplets to the beetle's mouth. Furthermore, the cactus *Opuntia microdasys*, which grows in the Chiu Wahwa Desert, collects water from fog with its razor blades. These blades have microspores at the tip with higher imperfections than the end areas, leading to variable wettability. Similar observations have been reported for the native grass of the Namib Desert, called *Stipagrostis sabulicola*, with hard stems up to 2 m tall [153,154]. This plant can guide water owing to the parallel grooves of the plant axis. *Cotula fallax* can also collect fog owing to the three-dimensional placement of its delicate leaves and hairs that cover it. The Sri Lankan spider *Uloborus walckenaerius* accomplishes this using silk made of twisted knots of nanofibrils.

In general, Fig. 14 depicts the path of using surfaces with various CA patterns. Based on this figure, it is concluded that using a hybrid surface is a promising method to control multiphase flow behavior in both gravity and microgravity conditions, and that by using this type of surface, we can control multiphase flow according to our requirements in different applications.

7. Conclusions

A comprehensive review of SH surfaces is presented to provide an understanding of the physics of such surfaces as well as their relevant theories, artificial surfaces, and fabrication methods. The review includes several examples of naturally occurring SH surfaces and discusses their properties. It further reveals the significant potential of SH surfaces in a number of applications pertinent to the petroleum industry, leading to its performance enhancement. For instance, SH surfaces can improve the oil/water separation process. Furthermore, the application of offshore systems such as floating solar cells as an auxiliary energy source is growing, and a large part of oil extraction and refining plants is in the form of offshore rigs. The use of SH surfaces reduces the formation of liquid wall films over equipment, which facilitates the control of the performance of offshore solar cells. Furthermore, since petrochemical equipment is constantly exposed to corrosion, it has been shown that the use of hydrophobic surfaces could help protect the equipment. It has been argued that applying SH surfaces could aid petroleum-related operations in cold climates by preventing gelatinization of crude oil and freezing the transmission line. Importantly, it has been shown that using SH surfaces allows water collection in deep oilfield drilling and promotes decrease of drag. It has also been shown that surface morphology and contact/sliding angles are related. Nevertheless, the fabrication of these surfaces remains quite expensive, and hence there is a pressing need to develop manufacturing methods to fabricate SH surfaces at a lower price. Another drawback is that the application of these surfaces in some industries leads to a pressure drop while maintaining their properties, which is dependent upon the environmental conditions. Thus, further studies are required to make SH surfaces more resistant to environmental conditions and reduce the resultant pressure drop.

As a future direction, the authors propose combining SH surfaces with hydrophilic surfaces for use in a variety of applications, owing to the beneficial presence of interactions between superhydrophobicity and hydrophilicity forces. In particular, comprehensive studies are required on hydrophobic-hydrophilic hybrid surfaces.

Declaration of Competing Interest

The authors declare that they have no known competing financial interests or personal relationships that could have appeared to influence the work reported in this paper.

References

[1] E. Sadeghinezhad, M.A.Q. Siddiqui, H. Roshan, K. Regenauer-Lieb, On the interpretation of contact angle for geomaterial wettability: contact area versus three-phase contact line, J. Pet. Sci. Eng. 195 (2020) 107579.

[2] M. Azadi Tabar, M.H. Ghazanfari, A. Dehghan Monfared, Compare numerical modeling and improved understanding of dynamic sessile drop contact angle analysis in Liquid-Solid-Gas system, J. Pet. Sci. Eng. 184 (2020) 106552.
[3] S. Wang, L. Jiang, Definition of superhydrophobic states, Adv. Mater. 19 (2007) 3423–3424.
[4] H.K. Webb, R.J. Crawford, E.P. Ivanova, Wettability of natural superhydrophobic surfaces, Adv. Colloid Interface Sci. 210 (2014) 58–64.
[5] K.L. Mittal, Advances in Contact Angle, Wettability and Adhesion, Volume 3, Wiley, 2018.
[6] D. Bonn, J. Eggers, J. Indekeu, J. Meunier, E. Rolley, Wetting and spreading, Rev. Mod. Phys. 81 (2009) 739–805.
[7] G. Kumar, K.N. Prabhu, Review of non-reactive and reactive wetting of liquids on surfaces, Adv. Colloid Interface Sci. 133 (2007) 61–89.
[8] S, Banerjee, Simple derivation of Young, Wenzel and Cassie-Baxter equations and its interpretations, arXiv preprint arXiv:0808.1460, (2008).
[9] G. Whyman, E. Bormashenko, T. Stein, The rigorous derivation of Young, Cassie-Baxter and Wenzel equations and the analysis of the contact angle hysteresis phenomenon, Chem. Phys. Lett. 450 (2008) 355–359.
[10] E, Bormashenko, Y, Boruvka–Neumann, Wenzel and Cassie–Baxter equations as the transversality conditions for the variational problem of wetting, Colloids and Surfaces A: Physicochemical and Engineering Aspects, 345 (2009) 163-165.
[11] T. Young, III, Philosophical transactions of the royal society of London, An essay on the cohesion of fluids, 1805, pp. 65–87.
[12] K. Liu, X. Yao, L. Jiang, Recent developments in bio-inspired special wettability, Chem. Soc. Rev. 39 (2010) 3240–3255.
[13] W.J. Jasper, N. Anand, A generalized variational approach for predicting contact angles of sessile nano-droplets on both flat and curved surfaces, J. Mol. Liq. 281 (2019) 196–203.
[14] S.H. Kim, Fabrication of superhydrophobic surfaces, J. Adhes. Sci. Technol. 22 (2008) 235–250.
[15] A.M. Mohamed, A.M. Abdullah, N.A. Younan, Corrosion behavior of superhydrophobic surfaces: a review, Arab. J. Chem. 8 (2015) 749–765.
[16] B. Bhushan, Y.C. Jung, K. Koch, Micro-, nano-and hierarchical structures for superhydrophobicity, self-cleaning and low adhesion, Philos. Trans. R. Soc. A Math. Phys. Eng. Sci. 367 (2009) 1631–1672.
[17] J. Bico, U. Thiele, D. Quéré, Wetting of textured surfaces, Colloids Surf. A Physicochem. Eng. Asp 206 (2002) 41–46.
[18] K. Satoh, H. Nakazumi, M. Morita, Preparation of super-water-repellent fluorinated inorganic-organic coating films on nylon 66 by the sol-gel method using microphase separation, J. Sol-Gel Sci. Technol. 27 (2003) 327–332.
[19] W. Barthlott, C. Neinhuis, Purity of the sacred lotus, or escape from contamination in biological surfaces, Planta 202 (1997) 1–8.
[20] B. Bhushan, Y.C. Jung, Wetting, adhesion and friction of superhydrophobic and hydrophilic leaves and fabricated micro/nanopatterned surfaces, J. Phys. Condens. Matter 20 (2008) 225010.
[21] P. Roach, N.J. Shirtcliffe, M.I. Newton, Progess in superhydrophobic surface development, Soft Matter. 4 (2008) 224–240.
[22] C. Neinhuis, W. Barthlott, Characterization and distribution of water-repellent, self-cleaning plant surfaces, Ann. Bot. 79 (1997) 667–677.
[23] D. McMullan, Scanning electron microscopy 1928–1965, Scanning 17 (1995) 175–185.
[24] C. Hu, W. Chen, T. Li, Y. Ding, H. Yang, S. Zhao, E.A. Tsiwah, X. Zhao, Y. Xie, Constructing non-fluorinated porous superhydrophobic SiO2-based films with robust mechanical properties, Colloids Surf. A Physicochem. Eng. Asp 551 (2018) 65–73.
[25] M. Barberoglou, V. Zorba, E. Stratakis, E. Spanakis, P. Tzanetakis, S.H. Anastasiadis, C. Fotakis, Bio-inspired water repellent surfaces produced by ultrafast laser structuring of silicon, Appl. Surf. Sci. 255 (2009) 5425–5429.
[26] D.-H. Kim, D.-H. Lee, Effect of irradiation on the surface morphology of nanostructured superhydrophobic surfaces fabricated by ion beam irradiation, Appl. Surf. Sci. 477 (2019) 154–158.
[27] Y. Gao, J. Wang, W. Xia, X. Mou, Z. Cai, Reusable hydrophilic-superhydrophobic patterned weft backed woven fabric for high-efficiency water-harvesting application, ACS Sustain. Chem. Eng. 6 (2018) 7216–7220.
[28] A.R. Betz, J. Jenkins, C.-J.-C. Kim, D. Attinger, Boiling heat transfer on superhydrophilic, superhydrophobic, and superbiphilic surfaces, Int. J. Heat Mass Transf. 57 (2013) 733–741.
[29] P. Zhang, F.Y. Lv, A review of the recent advances in superhydrophobic surfaces and the emerging energy-related applications, Energy 82 (2015) 1068–1087.
[30] C. Dietz, K. Rykaczewski, A.G. Fedorov, Y. Joshi, Visualization of droplet departure on a superhydrophobic surface and implications to heat transfer enhancement during dropwise condensation, Appl. Phys. Lett. 97 (2010) 033104.
[31] N.M. Nouri, M.S. Bakhsh, S. Sekhavat, Analysis of shear rate effects on drag reduction in turbulent channel flow with superhydrophobic wall, J. Hydrodyn. 25 (2013) 944–953.
[32] S. Barthwal, B. Lee, S.-H. Lim, Fabrication of robust and durable slippery anti-icing coating on textured superhydrophobic aluminum surfaces with infused silicone oil, Appl. Surf. Sci. 496 (2019) 143677.
[33] J. Lomga, P. Varshney, D. Nanda, M. Satapathy, S.S. Mohapatra, A. Kumar, Fabrication of durable and regenerable superhydrophobic coatings with excellent self-cleaning and anti-fogging properties for aluminium surfaces, J. Alloy. Compd. 702 (2017) 161–170.
[34] S. Li, J. Huang, Z. Chen, G. Chen, Y. Lai, A review on special wettability textiles: theoretical models, fabrication technologies and multifunctional applications, J. Mater. Chem. A 5 (2017) 31–55.
[35] W. Dou, J. Wu, T. Gu, P. Wang, D. Zhang, Preparation of super-hydrophobic micro-needle CuO surface as a barrier against marine atmospheric corrosion, Corros. Sci. 131 (2018) 156–163.
[36] C.-H. Xue, S.-T. Jia, J. Zhang, J.-Z. Ma, Large-area fabrication of superhydrophobic surfaces for practical applications: an overview, Sci. Technol. Adv. Mater. 11 (2010) 033002.
[37] M.R. Akhtari, N. Karimi, Thermohydraulic analysis of a microchannel with varying superhydrophobic roughness, Appl. Therm. Eng. 172 (2020) 115147.
[38] B. Wang, S. Peng, Y. Wang, X. Li, K. Zhang, C. Liu, A non-fluorine method for preparing multifunctional robust superhydrophobic coating with applications in photocatalysis, flame retardance, and oil–water separation, New J. Chem. 43 (2019) 7471–7481.
[39] F.E. Budde, Self-cleaning, odor reducing, and water shedding properties of titanium dioxide (TiO2) photocatalytic oxidizing coatings, Met. Finish. 108 (2010) 34–36.
[40] A. Mills, A. Lepre, N. Elliott, S. Bhopal, I.P. Parkin, S.A. O'Neill, Characterisation of the photocatalyst Pilkington Activ™: a reference film photocatalyst?, J Photochem. Photobiol. A Chem. 160 (2003) 213–224.
[41] M. Elbahri, D. Paretkar, K. Hirmas, S. Jebril, R. Adelung, Anti-lotus effect for nanostructuring at the leidenfrost temperature, Adv. Mater. 19 (2007) 1262–1266.

[42] M.H. Imanieh, Y. Vahidshad, P. Nourpour, S. Shakesi, K. Shabani, Different morphologies of tio2 nanostructures in acidic and basic sol–gel method, Nano 05 (2010) 279–285.
[43] I. Nakamura, N. Negishi, S. Kutsuna, T. Ihara, S. Sugihara, K. Takeuchi, Role of oxygen vacancy in the plasma-treated TiO2 photocatalyst with visible light activity for NO removal, J. Mol. Catal. A Chem. 161 (2000) 205–212.
[44] A.A. Keller, V. Broje, K. Setty, Effect of advancing velocity and fluid viscosity on the dynamic contact angle of petroleum hydrocarbons, J. Pet. Sci. Eng. 58 (2007) 201–206.
[45] R.J. Good, A thermodynamic derivation of Wenzel's modification of young's equation for contact angles; together with a theory of hysteresis1, J. Am. Chem. Soc. 74 (1952) 5041–5042.
[46] D.Y. Kwok, A.W. Neumann, Contact angle measurement and contact angle interpretation, Adv. Colloid Interface Sci. 81 (1999) 167–249.
[47] L.T. Popoola, A.S. Grema, G.K. Latinwo, B. Gutti, A.S. Balogun, Corrosion problems during oil and gas production and its mitigation, Int. J. Industrial Chem. 4 (2013) 35.
[48] A.M.A. Mohamed, A.M. Abdullah, N.A. Younan, Corrosion behavior of superhydrophobic surfaces: a review, Arab. J. Chem. 8 (2015) 749–765.
[49] D. Zhang, L. Wang, H. Qian, X. Li, Superhydrophobic surfaces for corrosion protection: a review of recent progresses and future directions, J. Coat. Technol. Res. 13 (2016) 11–29.
[50] E. Vazirinasab, R. Jafari, G. Momen, Application of superhydrophobic coatings as a corrosion barrier: a review, Surf. Coat. Technol. 341 (2018) 40–56.
[51] T. Liu, S. Chen, S. Cheng, J. Tian, X. Chang, Y. Yin, Corrosion behavior of super-hydrophobic surface on copper in seawater, Electrochim. Acta 52 (2007) 8003–8007.
[52] J. Jeevahan, M. Chandrasekaran, G. Britto Joseph, R.B. Durairaj, G. Mageshwaran, Superhydrophobic surfaces: a review on fundamentals, applications, and challenges, J. Coat. Technol. Res. 15 (2018) 231–250.
[53] R. Ramachandran, M. Nosonovsky, Coupling of surface energy with electric potential makes superhydrophobic surfaces corrosion-resistant, PCCP 17 (2015) 24988–24997.
[54] K. Watanabe, Y. Udagawa, H. Udagawa, Drag reduction of Newtonian fluid in a circular pipe with a highly water-repellent wall, J. Fluid Mech. 381 (1999) 225–238.
[55] Y. Luo, W. Song, X. Wang, Water repellent/wetting characteristics of various bio-inspired morphologies and fluid drag reduction testing research, Micron 82 (2016) 9–16.
[56] J. Fink, Chapter 12 - Drag reducers, in: J. Fink (Ed.), Petroleum Engineer's Guide to Oil Field Chemicals and Fluids (Second Edition), Gulf Professional Publishing, Boston, 2015, pp. 393–403.
[57] Z.-Y. Deng, W. Wang, L.-H. Mao, C.-F. Wang, S. Chen, Versatile superhydrophobic and photocatalytic films generated from TiO2–SiO2@PDMS and their applications on fabrics, J. Mater. Chem. A 2 (2014) 4178–4184.
[58] H. Dong, M. Cheng, Y. Zhang, H. Wei, F. Shi, Extraordinary drag-reducing effect of a superhydrophobic coating on a macroscopic model ship at high speed, J. Mater. Chem. A 1 (2013) 5886–5891.
[59] S. Zhang, X. Ouyang, J. Li, S. Gao, S. Han, L. Liu, H. Wei, Underwater drag-reducing effect of superhydrophobic submarine model, Langmuir 31 (2015) 587–593.
[60] Z. Li, J. Marlena, D. Pranantyo, B.L. Nguyen, C.H. Yap, A porous superhydrophobic surface with active air plastron control for drag reduction and fluid impalement resistance, J. Mater. Chem. A 7 (2019) 16387–16396.
[61] Y. Jeung, K. Yong, Underwater superoleophobicity of a superhydrophilic surface with unexpected drag reduction driven by electrochemical water splitting, Chem. Eng. J. 381 (2020) 122734.
[62] C.C, Ryerson, Assessment of superstructure ice protection as applied to offshore oil operations safety, in, 2009.
[63] C.C. Ryerson, Ice protection of offshore platforms, Cold Reg. Sci. Technol. 65 (2011) 97–110.
[64] C.C, Ryerson, S.T, Tripp, Managing Offshore Superstructure Icing, in: OTC Arctic Technology Conference, 2014, pp. OTC-24663-MS.
[65] R.D. Brown, P. Roebber, C.C. Centre, M.E.P. Company, The ice accretion problem in canadian waters related to offshore energy and transportation, Atmospheric Environment Service, Climatological Services Division, 1985.
[66] O, Mycyk, Session 2: Icing Case Studies, in: Proceedings International Workshop on Offshore Winds and Icing, 1985, pp. 388-389.
[67] L. Mishchenko, B. Hatton, V. Bahadur, J.A. Taylor, T. Krupenkin, J. Aizenberg, Design of ice-free nanostructured surfaces based on repulsion of impacting water droplets, ACS Nano 4 (2010) 7699–7707.
[68] L. Cao, A.K. Jones, V.K. Sikka, J. Wu, D. Gao, Anti-icing superhydrophobic coatings, Langmuir 25 (2009) 12444–12448.
[69] Y. Shen, J. Tao, H. Tao, S. Chen, L. Pan, T. Wang, Anti-icing potential of superhydrophobic ti6al4v surfaces: ice nucleation and growth, Langmuir 31 (2015) 10799–10806.
[70] J. Zhang, C. Gu, J. Tu, Robust slippery coating with superior corrosion resistance and anti-icing performance for AZ31B Mg Alloy Protection, ACS Appl. Mater. Interfaces 9 (2017) 11247–11257.
[71] M, Khodaei, Introductory Chapter: Superhydrophobic Surfaces-Introduction and Applications, in: Superhydrophobic Surfaces-Fabrications to Practical Applications, IntechOpen, 2019.
[72] J. Tang, H. Quan, J. Ye, Photocatalytic properties and photoinduced hydrophilicity of surface-fluorinated TiO2, Chem. Mater. 19 (2007) 116–122.
[73] E. Baldini, L. Chiodo, A. Dominguez, M. Palummo, S. Moser, M. Yazdi-Rizi, G. Auböck, B.P.P. Mallett, H. Berger, A. Magrez, C. Bernhard, M. Grioni, A. Rubio, M. Chergui, Strongly bound excitons in anatase TiO2 single crystals and nanoparticles, Nat. Commun. 8 (2017) 13.
[74] L. Zhang, Z. Dai, G. Zheng, Z. Yao, J. Mu, Superior visible light photocatalytic performance of reticular BiVO 4 synthesized via a modified sol–gel method, RSC Adv. 8 (2018) 10654–10664.
[75] Y. Kameya, H. Yabe, Optical and superhydrophilic characteristics of TiO2 coating with subwavelength surface structure consisting of spherical nanoparticle aggregates, Coatings 9 (2019) 547.
[76] A. Sarkar, G.G. Khan, The formation and detection techniques of oxygen vacancies in titanium oxide-based nanostructures, Nanoscale 11 (2019) 3414–3444.
[77] J.H. Worrell, Inorganic Chemistry: an industrial and environmental perspective (Swaddle, T. W.), J. Chem. Educ. 74 (1997) 1399.
[78] M. Ohring, Chapter 1 - a Review of Materials Science, in: M. Ohring (Ed.), Materials Science of Thin Films (Second Edition) , Academic Press, San Diego, 2002, pp. 1–56.
[79] R.N. Wenzel, Resistance of solid surfaces to wetting by water, Ind. Eng. Chem. 28 (1936) 988–994.
[80] C, Temizel, M, Irani, C.H, Canbaz, Y, Palabiyik, R, Moreno, A, Balikcioglu, J.M, Diaz, G, Zhang, J, Wang, A, Alkouh, Technical and Economical Aspects of Use of Solar Energy in Oil & Gas Industry in the Middle East, in: SPE International Heavy Oil Conference and Exhibition, 2018, pp. D022S028R001.

[81] M. Absi Halabi, A. Al-Qattan, A. Al-Otaibi, Application of solar energy in the oil industry—current status and future prospects, Renew. Sustain. Energy Rev. 43 (2015) 296–314.
[82] R, Meyer, E, Attanasi, P, Freeman, Heavy oil and natural bitumen resources in geological basins of the world. Open File-Report 2007-1084, US Geological Survey, Washington, DC. pubs. usgs. gov/of/2007/1084/(accessed November 29, 2010), (2007).
[83] M. Cid, N. Stem, C. Brunetti, A.F. Beloto, C.A.S. Ramos, Improvements in anti-reflection coatings for high-efficiency silicon solar cells, Surf. Coat. Technol. 106 (1998) 117–120.
[84] K. Hasan, S.B. Yousuf, M.S.H.K. Tushar, B.K. Das, P. Das, M.S. Islam, Effects of different environmental and operational factors on the PV performance: a comprehensive review, Energy Sci. Eng. 10 (2022) 656–675.
[85] A. Urbina, The balance between efficiency, stability and environmental impacts in perovskite solar cells: a review, J. Phys. Energy 2 (2020) 022001.
[86] M.R. Maghami, H. Hizam, C. Gomes, M.A. Radzi, M.I. Rezadad, S. Hajighorbani, Power loss due to soiling on solar panel: a review, Renew. Sustain. Energy Rev. 59 (2016) 1307–1316.
[87] U. Mehmood, F.A. Al-Sulaiman, B.S. Yilbas, B. Salhi, S.H.A. Ahmed, M.K. Hossain, Superhydrophobic surfaces with antireflection properties for solar applications: a critical review, Sol. Energy Mater. Sol. Cells 157 (2016) 604–623.
[88] D.M. Giolando, Nano-crystals of titanium dioxide in aluminum oxide: a transparent self-cleaning coating applicable to solar energy, Sol. Energy 97 (2013) 195–199.
[89] Y.-B. Park, H. Im, M. Im, Y.-K. Choi, Self-cleaning effect of highly water-repellent microshell structures for solar cell applications, J. Mater. Chem. 21 (2011) 633–636.
[90] J. Son, S. Kundu, L.K. Verma, M. Sakhuja, A.J. Danner, C.S. Bhatia, H. Yang, A practical superhydrophilic self cleaning and antireflective surface for outdoor photovoltaic applications, Sol. Energy Mater. Sol. Cells 98 (2012) 46–51.
[91] C. Gao, Z. Sun, K. Li, Y. Chen, Y. Cao, S. Zhang, L. Feng, Integrated oil separation and water purification by a double-layer TiO2-based mesh, Energ. Environ. Sci. 6 (2013) 1147–1151.
[92] C.R. Crick, J.A. Gibbins, I.P. Parkin, Superhydrophobic polymer-coated copper-mesh; membranes for highly efficient oil–water separation, J. Mater. Chem. A 1 (2013) 5943–5948.
[93] B. Chen, J. Qiu, E. Sakai, N. Kanazawa, R. Liang, H. Feng, Robust and superhydrophobic surface modification by a "Paint + Adhesive" method: applications in self-cleaning after oil contamination and oil-water separation, ACS Appl. Mater. Interfaces 8 (2016) 17659–17667.
[94] F. Bento, Complexity in the oil and gas industry: a study into exploration and exploitation in integrated operations, J. Open Innovation: Technol. Market, and Complexity 4 (2018) 11.
[95] Y. Zhu, C.Y. Tso, T.C. Ho, M.K.H. Leung, S. Yao, H.H. Qiu, Heat transfer enhancement on tube surfaces with biphilic nanomorphology, Appl. Therm. Eng. 180 (2020) 115778.
[96] J. Zhao, H. Dong, X. Wang, X. Fu, Research on heat transfer characteristic of crude oil during the tubular heating process in the floating roof tank, Case Studies in Thermal, Engineering 10 (2017) 142–153.
[97] X. Ma, S. Wang, Z. Lan, B. Peng, H.B. Ma, P. Cheng, Wetting mode evolution of steam dropwise condensation on superhydrophobic surface in the presence of noncondensable gas, J. Heat Transfer 134 (2011).
[98] H.W. Hu, G.H. Tang, D. Niu, Experimental investigation of condensation heat transfer on hybrid wettability finned tube with large amount of noncondensable gas, Int. J. Heat Mass Transf. 85 (2015) 513–523.
[99] H.W. Hu, G.H. Tang, D. Niu, Experimental investigation of convective condensation heat transfer on tube bundles with different surface wettability at large amount of noncondensable gas, Appl. Therm. Eng. 100 (2016) 699–707.
[100] P.S. Mahapatra, A. Ghosh, R. Ganguly, C.M. Megaridis, Key design and operating parameters for enhancing dropwise condensation through wettability patterning, Int. J. Heat Mass Transf. 92 (2016) 877–883.
[101] L. Guo, G.H. Tang, Dropwise condensation on bioinspired hydrophilic-slippery surface, RSC Adv. 8 (2018) 39341–39351.
[102] T.-Y. Zhang, L.-W. Mou, J.-Y. Zhang, L.-W. Fan, J.-Q. Li, A visualized study of enhanced steam condensation heat transfer on a honeycomb-like microporous superhydrophobic surface in the presence of a non-condensable gas, Int. J. Heat Mass Transf. 150 (2020) 119352.
[103] H. Yang, S. Wang, X. Wang, W. Chao, N. Wang, X. Ding, F. Liu, Q. Yu, T. Yang, Z. Yang, J. Li, C. Wang, G. Li, Wood-based composite phase change materials with self-cleaning superhydrophobic surface for thermal energy storage, Appl. Energy 261 (2020) 114481.
[104] T. Sun, H. Tan, D. Han, Q. Fu, L. Jiang, No platelet can adhere–largely improved blood compatibility on nanostructured superhydrophobic surfaces, Small 1 (2005) 959–963.
[105] I. Hejazi, J. Seyfi, E. Hejazi, G.M.M. Sadeghi, S.H. Jafari, H. A. Khonakdar, Investigating the role of surface micro/nano structure in cell adhesion behavior of superhydrophobic polypropylene/nanosilica surfaces, Colloids Surf. B Biointerfaces 127 (2015) 233–240.
[106] K. Ma, A. Li, S. Guo, J. Pang, Y. Xue, Z. Zhou, Techniques for improving the water-flooding of oil fields during the high water-cut stage, Oil Gas Sci. Technol. – Rev. IFP Energies nouvelles 74 (2019) 69.
[107] T. Wang, X. Hu, S. Dong, A general route to transform normal hydrophilic cloths into superhydrophobic surfaces, Chem. Commun. (2007) 1849–1851.
[108] J. Zimmermann, F.A. Reifler, G. Fortunato, L.-C. Gerhardt, S. Seeger, A. Simple, One-step approach to durable and robust superhydrophobic textiles, Adv. Funct. Mater. 18 (2008) 3662–3669.
[109] H. Bai, L. Wang, J. Ju, R. Sun, Y. Zheng, L. Jiang, Efficient water collection on integrative bioinspired surfaces with star-shaped wettability patterns, Adv. Mater. 26 (2014) 5025–5030.
[110] H. Zhu, Z. Guo, Hybrid engineered materials with high water-collecting efficiency inspired by Namib Desert beetles, Chem. Commun. 52 (2016) 6809–6812.
[111] X. Wang, J. Zeng, X. Yu, C. Liang, Y. Zhang, Water harvesting method via a hybrid superwettable coating with superhydrophobic and superhydrophilic nanoparticles, Appl. Surf. Sci. 465 (2019) 986–994.
[112] J. Lu, C.-V. Ngo, S.C. Singh, J. Yang, W. Xin, Z. Yu, C. Guo, Bioinspired hierarchical surfaces fabricated by femtosecond laser and hydrothermal method for water harvesting, Langmuir 35 (2019) 3562–3567.
[113] F. Wang, C. Liang, W. Yang, X. Zhang, Effects of frost thickness on dynamic defrosting on vertical hydrophobic and superhydrophobic fin surfaces, Energ. Buildings 223 (2020) 110134.
[114] L.B. Boinovich, A.M. Emelyanenko, V.K. Ivanov, A.S. Pashinin, Durable icephobic coating for stainless steel, ACS Appl. Mater. Interfaces 5 (2013) 2549–2554.
[115] S. Farhadi, M. Farzaneh, S.A. Kulinich, Anti-icing performance of superhydrophobic surfaces, Appl. Surf. Sci. 257 (2011) 6264–6269.
[116] Z.Z. Luo, Z.Z. Zhang, L.T. Hu, W.M. Liu, Z.G. Guo, H.J. Zhang, W.J. Wang, Stable bionic superhydrophobic coating surface fabricated by a conventional curing process, Adv. Mater. 20 (2008) 970–974.

[117] V.A. Ganesh, H.K. Raut, A.S. Nair, S. Ramakrishna, A review on self-cleaning coatings, J. Mater. Chem. 21 (2011) 16304–16322.
[118] S. Hajra, M. Sahu, R. Sahu, A.M. Padhan, P. Alagarsamy, H.-G. Kim, H. Lee, S. Oh, Y. Yamauchi, H.J. Kim, Significant effect of synthesis methodologies of metal-organic frameworks upon the additively manufactured dual-mode triboelectric nanogenerator towards self-powered applications, Nano Energy 98 (2022) 107253.
[119] S. Panda, S. Hajra, K. Mistewicz, P. In-na, M. Sahu, P.M. Rajaitha, H.J. Kim, Piezoelectric energy harvesting systems for biomedical applications, Nano Energy 100 (2022) 107514.
[120] J. Seo, S. Hajra, M. Sahu, H.J. Kim, Effect of cilia microstructure and ion injection upon single-electrode triboelectric nanogenerator for effective energy harvesting, Mater. Lett. 304 (2021) 130674.
[121] G. Wang, J. Zhou, M. Wang, Y. Zhang, Y. Zhang, Q. He, Superhydrophobic surface with aging resistance, excellent mechanical, restorable and droplet bounce properties, Soft Matter (2020).
[122] J. Li, C. Li, C. Li, Construction of plasma sprayed surfaces with various scales and the effect on hydrophobicity, Surf. Coat. Technol. 385 (2020) 125447.
[123] N.J. Shirtcliffe, G. McHale, S. Atherton, M.I. Newton, An introduction to superhydrophobicity, Adv. Colloid Interface Sci. 161 (2010) 124–138.
[124] X. Feng, L. Jiang, Design and creation of superwetting/antiwetting surfaces, Adv. Mater. 18 (2006) 3063–3078.
[125] X. Gao, X. Wang, X. Ouyang, C. Wen, Flexible Superhydrophobic and Superoleophilic MoS2 sponge for highly efficient oil-water separation, Sci. Rep. 6 (2016) 27207.
[126] N. Lv, X. Wang, S. Peng, L. Luo, R. Zhou, Superhydrophobic/superoleophilic cotton-oil absorbent: preparation and its application in oil/water separation, RSC Adv. 8 (2018) 30257–30264.
[127] Q. Li, Y. Yan, M. Yu, B. Song, S. Shi, Y. Gong, Synthesis of polymeric fluorinated sol–gel precursor for fabrication of superhydrophobic coating, Appl. Surf. Sci. 367 (2016) 101–108.
[128] M. Wang, M. Peng, Y.-X. Weng, Y.-D. Li, J.-B. Zeng, Toward durable and robust superhydrophobic cotton fabric through hydrothermal growth of ZnO for oil/water separation, Cellul. 26 (2019) 8121–8133.
[129] S. Feng, W. Luo, L. Wang, S. Zhang, N. Guo, M. Xu, Z. Zhao, D. Jia, X. Wang, L. Jia, Preparation and property of extremely stable superhydrophobic carbon fibers with core-shell structure, Carbon 150 (2019) 284–291.
[130] P. Varshney, D. Nanda, M. Satapathy, S.S. Mohapatra, A. Kumar, A facile modification of steel mesh for oil–water separation, New J. Chem. 41 (2017) 7463–7471.
[131] D. Zhang, L. Li, Y. Wu, W. Sun, J. Wang, H. Sun, One-step method for fabrication of superhydrophobic and superoleophilic surface for water-oil separation, Colloids Surf. A Physicochem. Eng. Asp 552 (2018) 32–38.
[132] Y. Liu, K. Zhang, W. Yao, C. Zhang, Z. Han, L. Ren, A facile electrodeposition process for the fabrication of superhydrophobic and superoleophilic copper mesh for efficient oil-water separation, Ind. Eng. Chem. Res. 55 (2016) 2704–2712.
[133] J. Yong, Q. Yang, C. Guo, F. Chen, X. Hou, A review of femtosecond laser-structured superhydrophobic or underwater superoleophobic porous surfaces/materials for efficient oil/water separation, RSC Adv. 9 (2019) 12470–12495.
[134] A. Pozzato, S.D. Zilio, G. Fois, D. Vendramin, G. Mistura, M. Belotti, Y. Chen, M. Natali, Superhydrophobic surfaces fabricated by nanoimprint lithography, Microelectron. Eng. 83 (2006) 884–888.
[135] N.J. Shirtcliffe, G. McHale, S. Atherton, M.I. Newton, An introduction to superhydrophobicity, Adv. Colloid Interface Sci. 161 (2010) 124–138.
[136] T.T. Isimjan, T. Wang, S. Rohani, A novel method to prepare superhydrophobic, UV resistance and anti-corrosion steel surface, Chem. Eng. J. 210 (2012) 182–187.
[137] J. Wang, A. Wang, Acetylated modification of kapok fiber and application for oil absorption, Fibers Polym. 14 (2013) 1834–1840.
[138] Z. Wang, Q. Li, Z. She, F. Chen, L. Li, Low-cost and large-scale fabrication method for an environmentally-friendly superhydrophobic coating on magnesium alloy, J. Mater. Chem. 22 (2012) 4097–4105.
[139] X. Hou, F. Zhou, B. Yu, W. Liu, Superhydrophobic zinc oxide surface by differential etching and hydrophobic modification, Mater. Sci. Eng. A 452–453 (2007) 732–736.
[140] Y. Qing, C. Long, K. An, C. Hu, C. Liu, Sandpaper as template for a robust superhydrophobic surface with self-cleaning and anti-snow/icing performances, J. Colloid Interface Sci. 548 (2019) 224–232.
[141] M. Pei, C. Pan, D. Wu, P. Liu, Surface hydrophilic-hydrophobic reversal coatings of polydimethylsiloxane-palygorskite nanosponges, Appl. Clay Sci. 189 (2020) 105546.
[142] F. Wang, Y. Zhou, W. Yang, M. Ni, X. Zhang, C. Liang, Anti-frosting performance of sprayable superhydrophobic coating suitable for outdoor coil of air source heat pump, Appl. Therm. Eng. 169 (2020) 114967.
[143] J.-Y. Shiu, C.-W. Kuo, P. Chen, C.-Y. Mou, Fabrication of tunable superhydrophobic surfaces by nanosphere lithography, Chem. Mater. 16 (2004) 561–564.
[144] B. Bhushan, Y.C. Jung, Biomimetics inspired surfaces for superhydrophobicity, self-cleaning, low adhesion, and drag reduction, in: B. Bhushan (Ed.), Nanotribology and Nanomechanics II: Nanotribology, Biomimetics, and Industrial Applications, Springer, Berlin Heidelberg, Berlin, Heidelberg, 2011, pp. 533–699.
[145] B. Bhushan, Y.C. Jung, Natural and biomimetic artificial surfaces for superhydrophobicity, self-cleaning, low adhesion, and drag reduction, Prog. Mater Sci. 56 (2011) 1–108.
[146] M.A. Aegerter, R. Almeida, A. Soutar, K. Tadanaga, H. Yang, T. Watanabe, Coatings made by sol–gel and chemical nanotechnology, J. Sol-Gel Sci. Technol. 47 (2008) 203–236.
[147] N. Miljkovic, R. Enright, E.N. Wang, Modeling and optimization of superhydrophobic condensation, J. Heat Transfer 135 (2013).
[148] J, Stoddard, J, Crockett, D, Maynes, Droplet Train Impingement on Superhydrophobic Surfaces, in: APS Division of Fluid Dynamics Meeting Abstracts, 2014, pp. D13.004.
[149] R. Mohammadi, J. Wassink, A. Amirfazli, Effect of surfactants on wetting of super-hydrophobic surfaces, Langmuir 20 (2004) 9657–9662.
[150] S.M. Mousavi, B.J. Lee, Investigation of bubble structure in a microchannel under microgravity conditions: effects of discontinuous wettability with dynamic contact angle, Acta. Astronaut. 201 (2022) 394–400.
[151] S.M. Mousavi, F. Sotoudeh, B.J. Lee, M.-R. Paydari, N. Karimi, Effect of hybrid wall contact angles on slug flow behavior in a T-junction microchannel: a numerical study, Colloids Surf. A Physicochem. Eng. Asp 650 (2022) 129677.
[152] F. Sotoudeh, R. Kamali, S.M. Mousavi, N. Karimi, B.J. Lee, D. Khojasteh, Understanding droplet collision with superhydrophobic-hydrophobic–hydrophilic hybrid surfaces, Colloids Surf. A Physicochem. Eng. Asp 614 (2021) 126140.
[153] T. Darmanin, F. Guittard, Superhydrophobic and superoleophobic properties in nature, Mater. Today 18 (2015) 273–285.

[154] K. Yin, H. Du, X. Dong, C. Wang, J.-A. Duan, J. He, A simple way to achieve bioinspired hybrid wettability surface with micro/nanopatterns for efficient fog collection, Nanoscale 9 (2017) 14620–14626.
[155] D.O. Njobuenwu, R.H. Gumus, Determination of contact angle from contact area of liquid droplet spreading on solid substrate, Leonardo Electronic J. Practices and Technol. 10 (2007) 29–38.
[156] A.K. Kota, G. Kwon, A. Tuteja, The design and applications of superomniphobic surfaces, NPG Asia Mater. 6 (2014) e109–e.
[157] C. Hao, Y. Liu, X. Chen, J. Li, M. Zhang, Y. Zhao, Z. Wang, Bioinspired interfacial materials with enhanced drop mobility: from fundamentals to multifunctional applications, Small 12 (2016) 1825–1839.
[158] D. Khojasteh, M. Kazerooni, S. Salarian, R. Kamali, Droplet impact on superhydrophobic surfaces: a review of recent developments, J. Ind. Eng. Chem. 42 (2016) 1–14.
[159] M. Kumar, R. Bhardwaj, Wetting characteristics of Colocasia esculenta (Taro) leaf and a bioinspired surface thereof, Sci. Rep. 10 (2020) 935.
[160] G. Carbone, L. Mangialardi, Hydrophobic properties of a wavy rough substrate, The, Eur. Phys. J. E 16 (2005) 67–76.
[161] R. Crawford, E. Ivanova, Nat. Superhydrophobic Surfaces (2015) 7–25.
[162] F, Geyer, M, D'Acunzi, A, Sharifi-Aghili, A, Saal, N, Gao, A, Kaltbeitzel, T.-F, Sloot, R, Berger, H.-J, Butt, D, Vollmer, When and how self-cleaning of superhydrophobic surfaces works, Science Advances, 6 eaaw9727.
[163] K.M.T. Negara, I.N.G. Wardana, D. Widhiyanuriyawan, N. Hamidi, The role of the slope on taro leaf surface to produce electrical energy, IOP Conference Series: Mater. Sci. Eng. 494 (2019) 012084.
[164] J. Göhl, A. Mark, S. Sasic, F. Edelvik, An immersed boundary based dynamic contact angle framework for handling complex surfaces of mixed wettabilities, Int. J. Multiph. Flow 109 (2018) 164–177.
[165] A.R. Binesh, S.M. Mousavi, R. Kamali, Effect of temperature-dependency of Newtonian and non-Newtonian fluid properties on the dynamics of droplet impinging on hot surfaces, Int. J. Mod. Phys. C 26 (2015) 1550106.
[166] D. Khojasteh, S.M. Mousavi, R. Kamali, CFD analysis of Newtonian and non-Newtonian droplets impinging on heated hydrophilic and hydrophobic surfaces, Indian J. Phys. 91 (2017) 513–520.
[167] B.K. Tudu, A. Kumar, B. Bhushan, Facile approach to develop anti-corrosive superhydrophobic aluminium with high mechanical, chemical and thermal durability, Philos. Trans. R. Soc. A Math. Phys. Eng. Sci. 377 (2019) 20180272.
[168] D. Sebastian, C.-W. Yao, I. Lian, Mechanical durability of engineered superhydrophobic surfaces for anti-corrosion, Coatings 8 (2018) 162.
[169] A. Jha, K. Sarma, S. Chowdhury, Advancement of oil/water separating materials: merits and demerits in real-time applications, MOJ Poly Sci 1 (2017) 11–16.
[170] X. Yu, J. Zhao, C. Wu, B. Li, C. Sun, S. Huang, X. Tian, Highly durable antifogging coatings resistant to long-term airborne pollution and intensive UV irradiation, Mater. Des. 194 (2020) 108956.
[171] K. Van Maele, B. Merci, E. Dick, Comparative study of k-epsilon turbulence models in inert and reacting swirling flows, in: 33rd AIAA Fluid Dynamics Conference and Exhibit, American Institute of Aeronautics and Astronautics, 2003.
[172] M. Soltani Ayan, M. Entezari, S.F. Chini, Experiments on skin friction reduction induced by superhydrophobicity and Leidenfrost phenomena in a Taylor-Couette cell, Int. J. Heat Mass Transf. 132 (2019) 271–279.
[173] Y. Tuo, W. Chen, H. Zhang, P. Li, X. Liu, One-step hydrothermal method to fabricate drag reduction superhydrophobic surface on aluminum foil, Appl. Surf. Sci. 446 (2018) 230–235.
[174] L. Li, J. Zhu, S. Zhi, E. Liu, G. Wang, Z. Zeng, W. Zhao, Q. Xue, Study of adhesion and friction drag on a rough hydrophobic surface: Sandblasted aluminum, Phys. Fluids 30 (2018) 071903.
[175] L. Yin, H. Zhang, R. Weng, Z. Wu, X. Liu, Fabrication and drag reduction of the superoleophobic surface on a rotational gyroscope, Surf. Eng. 34 (2018) 165–171.
[176] P. Du, J. Wen, Z. Zhang, D. Song, A. Ouahsine, H. Hu, Maintenance of air layer and drag reduction on superhydrophobic surface, Ocean Eng. 130 (2017) 328–335.
[177] P. Wang, T. Yao, Z. Li, W. Wei, Q. Xie, W. Duan, H. Han, A superhydrophobic/electrothermal synergistically anti-icing strategy based on graphene composite, Compos. Sci. Technol. 198 (2020) 108307.
[178] S. Barthwal, S.-H. Lim, Rapid fabrication of a dual-scale micro-nanostructured superhydrophobic aluminum surface with delayed condensation and ice formation properties, Soft Matter. 15 (2019) 7945–7955.
[179] Y. Qi, Z. Yang, T. Chen, Y. Xi, J. Zhang, Fabrication of superhydrophobic surface with desirable anti-icing performance based on micro/nano-structures and organosilane groups, Appl. Surf. Sci. 501 (2020) 144165.
[180] X. Li, G. Wang, A.S. Moita, C. Zhang, S. Wang, Y. Liu, Fabrication of bio-inspired non-fluorinated superhydrophobic surfaces with anti-icing property and its wettability transformation analysis, Appl. Surf. Sci. 505 (2020) 144386.
[181] W. Hou, Y. Shen, J. Tao, Y. Xu, J. Jiang, H. Chen, Z. Jia, Anti-icing performance of the superhydrophobic surface with micro-cubic array structures fabricated by plasma etching, Colloids Surf. A Physicochem. Eng. Asp 586 (2020) 124180.
[182] J. Song, Y. Li, W. Xu, H. Liu, Y. Lu, Inexpensive and non-fluorinated superhydrophobic concrete coating for anti-icing and anti-corrosion, J. Colloid Interface Sci. 541 (2019) 86–92.
[183] J. Zhi, L.-Z. Zhang, Durable superhydrophobic surface with highly antireflective and self-cleaning properties for the glass covers of solar cells, Appl. Surf. Sci. 454 (2018) 239–248.
[184] Y. Liu, A. Das, S. Xu, Z. Lin, C. Xu, Z.L. Wang, A. Rohatgi, C.P. Wong, Hybridizing ZnO nanowires with micropyramid silicon wafers as superhydrophobic high-efficiency solar cells, Adv. Energy Mater. 2 (2012) 47–51.
[185] H.J. Gwon, Y. Park, C.W. Moon, S. Nahm, S.-J. Yoon, S.Y. Kim, H.W. Jang, Superhydrophobic and antireflective nanograss-coated glass for high performance solar cells, Nano Res. 7 (2014) 670–678.
[186] S. Sutha, S. Suresh, B. Raj, K.R. Ravi, Transparent alumina based superhydrophobic self–cleaning coatings for solar cell cover glass applications, Sol. Energy Mater. Sol. Cells 165 (2017) 128–137.
[187] W. Li, X. Tan, J. Zhu, P. Xiang, T. Xiao, L. Tian, A. Yang, M. Wang, X. Chen, Broadband antireflective and superhydrophobic coatings for solar cells, Mater. Today Energy 12 (2019) 348–355.
[188] Y, Liu, Y, Xiu, C.P, Wong, Micro/nano structure size effect on superhydrophobicity and anti reflection of single crystalline Si solar cells, in: 2010 Proceedings 60th Electronic Components and Technology Conference (ECTC), 2010, pp. 1719-1724.
[189] Y. Gao, I. Gereige, A. El Labban, D. Cha, T.T. Isimjan, P.M. Beaujuge, Highly transparent and UV-resistant superhydrophobic SiO2-Coated ZnO Nanorod Arrays, ACS Appl. Mater. Interfaces 6 (2014) 2219–2223.
[190] J. Xiong, S.N. Das, B. Shin, J.P. Kar, J.H. Choi, J.-M. Myoung, Biomimetic hierarchical ZnO structure with superhydrophobic and antireflective properties, J. Colloid Interface Sci. 350 (2010) 344–347.

[191] M. Wang, X. Gu, P. Ma, W. Zhang, D. Yu, P. Chang, X. Chen, D. Li, Microstructured superhydrophobic anti-reflection films for performance improvement of photovoltaic devices, Mater. Res. Bull. 91 (2017) 208–213.
[192] X. Zhang, J. Zhao, J. Mo, R. Sun, Z. Li, Z. Guo, Fabrication of superhydrophobic aluminum surface by droplet etching and chemical modification, Colloids Surf. A Physicochem. Eng. Asp 567 (2019) 205–212.
[193] S.A. Mahadik, F. Pedraza, R.S. Vhatkar, Silica based superhydrophobic coating for long-term industrial and domestic applications, J. Alloy. Compd. 663 (2016) 487–493.
[194] Y. Wang, C. Gao, W. Zhao, G. Zheng, Y. Ji, K. Dai, L. Mi, D. Zhang, C. Liu, C. Shen, Large-area fabrication and applications of patterned surface with anisotropic superhydrophobicity, Appl. Surf. Sci. (2020) 147027.
[195] J. Ma, X.Y. Zhang, D.P. Wang, D.Q. Zhao, D.W. Ding, K. Liu, W.H. Wang, Superhydrophobic metallic glass surface with superior mechanical stability and corrosion resistance, Appl. Phys. Lett. 104 (2014) 173701.
[196] S. Ji, P.A. Ramadhianti, T.-B. Nguyen, W.-D. Kim, H. Lim, Simple fabrication approach for superhydrophobic and superoleophobic Al surface, Microelectron. Eng. 111 (2013) 404–408.
[197] X. Liu, Y. Xu, K. Ben, Z. Chen, Y. Wang, Z. Guan, Transparent, durable and thermally stable PDMS-derived superhydrophobic surfaces, Appl. Surf. Sci. 339 (2015) 94–101.
[198] R. Sun, J. Zhao, Z. Li, N. Qin, J. Mo, Y. Pan, D. Luo, Robust superhydrophobic aluminum alloy surfaces with anti-icing ability, thermostability, and mechanical durability, Prog. Org. Coat. 147 (2020) 105745.
[199] Z. Lv, S. Yu, K. Song, X. Zhou, X. Yin, A two-step method fabricating a hierarchical leaf-like superamphiphobic PTFE/CuO coating on 6061Al, Prog. Org. Coat. 147 (2020) 105723.
[200] S. Barthwal, S. Barthwal, B. Singh, N. Bahadur Singh, Multifunctional and fluorine-free superhydrophobic composite coating based on PDMS modified MWCNTs/ZnO with self-cleaning, oil-water separation, and flame retardant properties, Colloids Surf. A Physicochem. Eng. Asp 597 (2020) 124776.
[201] Q. Pan, Y. Cao, W. Xue, D. Zhu, W. Liu, Picosecond laser-textured stainless steel superhydrophobic surface with an antibacterial adhesion property, Langmuir 35 (2019) 11414–11421.
[202] X. Zhang, Y. Guo, Z. Zhang, P. Zhang, Self-cleaning superhydrophobic surface based on titanium dioxide nanowires combined with polydimethylsiloxane, Appl. Surf. Sci. 284 (2013) 319–323.
[203] S. Sriram, A. Kumar, Separation of oil-water via porous PMMA/SiO2 nanoparticles superhydrophobic surface, Colloids Surf A Physicochem. Eng. Asp 563 (2019) 271–279.